

Mach2D com condições de contorno consistentes. Propulsão.

Guilherme Bertoldo

15 de Dezembro de 2012

Conteúdo

| | | |
|----------|---|-----------|
| 1 | Introdução | 1 |
| 2 | Condições de contorno | 1 |
| 2.1 | Exatas | 1 |
| 2.1.1 | Contorno norte | 2 |
| 2.1.2 | Contorno sul | 2 |
| 2.1.3 | Contorno leste | 2 |
| 2.1.4 | Contorno oeste | 2 |
| 2.2 | Esquema numérico consistente | 3 |
| 2.2.1 | Contorno norte | 3 |
| 2.2.2 | Contorno sul | 4 |
| 2.2.3 | Contorno leste | 5 |
| 2.2.4 | Contorno oeste | 5 |
| 2.3 | Esquema numérico inconsistente | 6 |
| 2.3.1 | Contorno norte | 6 |
| 2.3.2 | Contorno leste | 6 |
| 3 | Comparações | 6 |
| 3.1 | Parâmetros numéricos | 6 |
| 3.2 | Cd e Fd* | 7 |
| 3.3 | Campos u , v , T e p | 7 |
| 3.3.1 | Malha 56×20 | 7 |
| 3.3.2 | Malha 112×40 | 12 |
| 3.3.3 | Malha 224×80 | 16 |
| 3.3.4 | Malha 448×160 | 20 |
| 3.3.5 | Panorama geral | 24 |
| 4 | Conclusões | 24 |
| A | Revisões do código Mach2D-7-SVN-r201 | 25 |

1 Introdução

Este relatório compara os resultados obtidos com o código Mach2D-7-SVN-r195 (Branch: CBC), que utiliza um esquema numérico inconsistente¹ para as condições de contorno, com os resultados do código Mach2D-7-SVN-r201 (Branch: CBC), cujo esquema numérico foi corrigido.

O código base utilizado neste estudo é o Mach2D-7-SVN-r91 (Tag: Diego_version_for_linux), adaptado para Linux. Este código foi modificado para utilizar o esquema numérico inconsistente descrito na Seç. 2.3, que deu origem ao código Mach2D-7-SVN-r195 (Branch: CBC). Em seguida, o esquema numérico consistente, descrito na Seç. 2.2, foi implementado até se obter a versão Mach2D-7-SVN-r201 (Branch: CBC). Os detalhes da implementação são apresentados no Apêndice.

2 Condições de contorno

2.1 Exatas

Os contornos do domínio de cálculo são ilustrados na Fig. 1. As condições de contorno para as equações de Euler são apresentadas a seguir.

¹Um esquema numérico consistente é aquele que leva à equação exata a medida que a malha é refinada.

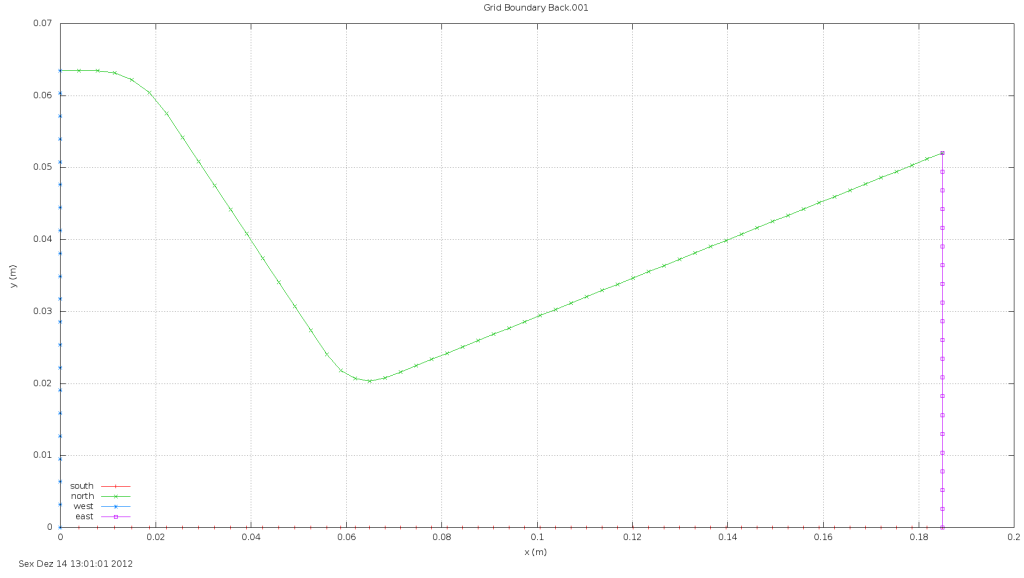


Figura 1: Contornos do domínio de cálculo

2.1.1 Contorno norte

$$(\hat{\mathbf{n}} \cdot \nabla)p = 0 \quad (1)$$

$$(\hat{\mathbf{n}} \cdot \nabla)T = 0 \quad (2)$$

$$\hat{\mathbf{n}} \cdot \mathbf{u} = 0 \quad (3)$$

2.1.2 Contorno sul

$$(\hat{\mathbf{n}} \cdot \nabla)u = 0 \quad (4)$$

$$v = 0 \quad (5)$$

$$(\hat{\mathbf{n}} \cdot \nabla)p = 0 \quad (6)$$

$$(\hat{\mathbf{n}} \cdot \nabla)T = 0 \quad (7)$$

2.1.3 Contorno leste

Escoamento localmente parabólico:

$$(\mathbf{u} \cdot \nabla)\phi = 0, \quad \phi \in \{p, T, u, v\} \quad (8)$$

2.1.4 Contorno oeste

$$\frac{\partial u}{\partial x} = 0, \quad (9)$$

$$v = 0, \quad (10)$$

$$T = T_{in}, \quad (11)$$

$$p = p_{in}, \quad (12)$$

onde

$$T_{in} = T_0 \left(1 - \frac{\gamma - 1}{2} \frac{u_{in}^2 + v_{in}^2}{\gamma R_g T_0} \right), \quad (13)$$

$$p_{in} = p_0 \left(1 + \frac{\gamma - 1}{2} M_{in}^2 \right)^{-\frac{\gamma}{\gamma - 1}} \quad (14)$$

e

$$M_{in}^2 = \frac{u_{in}^2 + v_{in}^2}{\gamma R_g T_{in}}. \quad (15)$$

2.2 Esquema numérico consistente

2.2.1 Contorno norte

1. Aproximações

Em termos das coordenadas ξ e η , as condições de contorno (1) e (2) ficam

$$-\beta_s \left(\frac{\partial \phi}{\partial \xi} \right)_s + \gamma_s \left(\frac{\partial \phi}{\partial \eta} \right)_s = 0, \quad \phi \in \{p, T\} \quad (16)$$

A derivada em relação a η é calculada através da aproximação

$$\left(\frac{\partial \phi}{\partial \eta} \right)_s = \frac{\phi_P - \phi_S}{\Delta \eta} \quad (17)$$

A derivada em relação a ξ depende do volume de controle. Para o volume de controle ($i=2, j=ny$), tem-se

$$\left(\frac{\partial \phi}{\partial \xi} \right)_s^m = \frac{\phi_E^m + \phi_{SE}^m - \phi_P^m - \phi_S^m}{2\Delta \xi}, \quad (18)$$

para o volume ($i=nx-1, j=ny$), tem-se

$$\left(\frac{\partial \phi}{\partial \xi} \right)_s^m = \frac{\phi_P^m + \phi_S^m - \phi_W^m - \phi_{SW}^m}{2\Delta \xi}, \quad (19)$$

e para os volumes ($2 < i < nx-1, j=ny$), tem-se

$$\left(\frac{\partial \phi}{\partial \xi} \right)_s^m = \frac{\phi_E^m + \phi_{SE}^m - \phi_W^m - \phi_{SW}^m}{4\Delta \xi}, \quad (20)$$

onde o índice m indica que se deve usar o valor da variável da última iteração.

Para se obter as aproximações para u e v , deve-se observar que o vetor velocidade \mathbf{u}_s deve ser tangente à superfície neste contorno. Como o contorno norte é uma linha de η constante, tem-se

$$\mathbf{u}_s = \lambda (\mathbf{E}_\xi)_s, \quad (21)$$

onde $(\mathbf{E}_\xi)_s$ é um vetor tangente à superfície e λ é um coeficiente a determinar.

Tendo em vista que

$$\mathbf{u}_s \rightarrow \mathbf{u}_s \quad (22)$$

a medida que a malha é refinada, o coeficiente λ é aproximado por

$$\lambda \simeq \text{sgn}(\mathbf{u}_s \cdot (\mathbf{E}_\xi)_s) \sqrt{\frac{u_s^2 + v_s^2}{(x_\xi)_s^2 + (y_\xi)_s^2}}. \quad (23)$$

Uma vez conhecido λ , tem-se

$$u_s = \frac{u_P + u_S}{2} = \lambda (x_\xi)_s, \quad (24)$$

$$v_s = \frac{v_P + v_S}{2} = \lambda (y_\xi)_s. \quad (25)$$

2. Extrapolações para os fictícios

Com base nas aproximações apresentadas acima, tem-se

$$u_P = -u_S + 2\lambda (x_\xi)_s \quad (26)$$

$$v_P = -v_S + 2\lambda (y_\xi)_s \quad (27)$$

$$T_P = T_S + \frac{\beta_s}{\gamma_s} \left(\frac{\partial T}{\partial \xi} \right)_s^m \Delta \eta \quad (28)$$

$$p_P = p_S + \frac{\beta_s}{\gamma_s} \left(\frac{\partial p}{\partial \xi} \right)_s^m \Delta \eta \quad (29)$$

3. Coeficientes dos sistemas lineares

Com base nas aproximações apresentadas acima, tem-se

$$A_P^u = 1, \quad A_S^u = 1, \quad b_P^u = 2\lambda (x_\xi)_s \quad (30)$$

$$A_P^v = 1, \quad A_S^v = 1, \quad b_P^v = 2\lambda (y_\xi)_s \quad (31)$$

$$A_P^T = 1, \quad A_S^T = -1, \quad b_P^T = \frac{\beta_s}{\gamma_s} \left(\frac{\partial T}{\partial \xi} \right)_s^m \Delta \eta \quad (32)$$

Os coeficientes do sistema linear para a correção da pressão são obtidos da equação

$$p_P = p_s + \frac{\beta_s}{\gamma_s} \left(\frac{\partial p}{\partial \xi} \right)_s^m \Delta \eta \quad (33)$$

com

$$p_P = p_P^* + p_P', \quad p_s = p_s^* + p_s'. \quad (34)$$

Como a condição

$$p_P^* = p_s^* + \frac{\beta_s}{\gamma_s} \left(\frac{\partial p}{\partial \xi} \right)_s^m \Delta \eta \quad (35)$$

é imposta a cada iteração, tem-se

$$p_P' = p_s', \quad (36)$$

logo

$$A_P^{p'} = 1, \quad A_S^{p'} = -1, \quad b_P^{p'} = 0. \quad (37)$$

2.2.2 Contorno sul

1. Aproximações

Como no contorno sul a malha é ortogonal, as condições de contorno (4), (6) e (7) são dadas por

$$\frac{\partial \phi}{\partial \eta} = 0, \quad \phi \in \{u, T, p\}, \quad (38)$$

cuja discretização é

$$\frac{\phi_N - \phi_P}{\Delta \eta} = 0, \quad \phi \in \{u, T, p\}, \quad (39)$$

A condição de contorno $v = 0$ é aproximada por

$$\frac{v_N + v_P}{2} = 0, \quad (40)$$

2. Extrapolações para os fictícios

Com base nas aproximações acima, tem-se

$$u_P = u_N \quad (41)$$

$$v_P = -v_N \quad (42)$$

$$T_P = T_N \quad (43)$$

$$p_P = p_N \quad (44)$$

3. Coeficientes dos sistemas lineares

Com base nas aproximações acima, tem-se

$$A_P^u = 1, \quad A_N^u = -1, \quad b_P^u = 0 \quad (45)$$

$$A_P^v = 1, \quad A_N^v = 1, \quad b_P^v = 0 \quad (46)$$

$$A_P^T = 1, \quad A_N^T = -1, \quad b_P^T = 0 \quad (47)$$

Os coeficientes do sistema linear para a correção da pressão são obtidos da equação

$$p_P = p_N \quad (48)$$

com

$$p_P = p_P^* + p_P', \quad p_N = p_N^* + p_N'. \quad (49)$$

Como a condição

$$p_P^* = p_N^* \quad (50)$$

é imposta a cada iteração, tem-se

$$p_P' = p_N', \quad (51)$$

logo

$$A_P^{p'} = 1, \quad A_N^{p'} = -1, \quad b_P^{p'} = 0. \quad (52)$$

2.2.3 Contorno leste

1. Aproximações

A condição de escoamento localmente parabólico

$$\mathbf{u} \cdot \nabla \phi = 0, \quad \phi \in \{p, T, u, v\}. \quad (53)$$

é escrita como

$$U_w \left(\frac{\partial \phi}{\partial \xi} \right)_w + V_w \left(\frac{\partial \phi}{\partial \eta} \right)_w, \quad \phi \in \{p, T, u, v\}. \quad (54)$$

A derivada em relação a ξ é aproximada por

$$\frac{\partial \phi}{\partial \xi} = \frac{\phi_P - \phi_W}{\Delta \xi}, \quad \phi \in \{p, T, u, v\}. \quad (55)$$

A derivada em relação a η depende do volume de controle. Para o volume de controle ($i=nx, j=2$), tem-se

$$\left(\frac{\partial \phi}{\partial \eta} \right)_w^m = \frac{\phi_N^m + \phi_{NW}^m - \phi_P^m - \phi_W^m}{2\Delta \eta}, \quad \phi \in \{p, T, u, v\}, \quad (56)$$

para o volume ($i=nx, j=ny-1$), tem-se

$$\left(\frac{\partial \phi}{\partial \eta} \right)_w^m = \frac{\phi_P^m + \phi_W^m - \phi_{SW}^m - \phi_S^m}{2\Delta \eta}, \quad \phi \in \{p, T, u, v\}, \quad (57)$$

e para os volumes ($i=nx, 2 < j < ny-1$), tem-se

$$\left(\frac{\partial \phi}{\partial \eta} \right)_w^m = \frac{\phi_N^m + \phi_{NW}^m - \phi_S^m - \phi_{SW}^m}{4\Delta \eta}, \quad \phi \in \{p, T, u, v\}, \quad (58)$$

onde o índice m indica que se deve usar o valor da variável da última iteração.

2. Extrapolações para os fictícios

Com base nas aproximações acima, tem-se

$$\phi_P = \phi_W - \frac{V_w}{U_w} \left(\frac{\partial \phi}{\partial \eta} \right)_w^m \Delta \xi, \quad \phi \in \{u, v, T, p\}. \quad (59)$$

3. Coeficientes dos sistemas lineares

Com base nas aproximações acima, tem-se

$$A_P^\phi = 1, \quad A_W^\phi = -1, \quad b_P^\phi = -\frac{V_w}{U_w} \left(\frac{\partial \phi}{\partial \eta} \right)_w^m \Delta \xi, \quad \phi \in \{u, v, T\}. \quad (60)$$

$$A_P^{\phi'} = 1, \quad A_W^{\phi'} = -1, \quad b_P^{\phi'} = 0. \quad (61)$$

2.2.4 Contorno oeste

1. Aproximações

A condição de contorno para u é aproximada por

$$\frac{\partial u}{\partial \xi} = \frac{u_E - u_P}{\Delta \xi} = 0. \quad (62)$$

Para as variáveis v , p e T é aplicada a aproximação

$$\frac{\phi_E + \phi_P}{2} = \phi_{in}. \quad (63)$$

2. Extrapolações para os fictícios

Com base nas aproximações acima

$$u_P = u_E \quad (64)$$

$$\phi_P = -\phi_E + 2\phi_{in}, \quad \phi \in \{v, T, p\}. \quad (65)$$

3. Coeficientes dos sistemas lineares

Com base nas aproximações acima, tem-se

$$A_P^u = 1, \quad A_E^u = -1, \quad b_P^u = 0, \quad (66)$$

$$A_P^\phi = 1, \quad A_E^\phi = 1, \quad b_P^\phi = 2\phi_{in}, \quad \phi \in \{v, T\}. \quad (67)$$

No caso da correção da pressão, segue-se a recomendação de Versteeg e Malalasekera[1] (ver pág. 207). Neste caso

$$A_P^{\phi'} = 1, \quad A_E^{\phi'} = 1, \quad b_P^{\phi'} = 0, \quad (68)$$

2.3 Esquema numérico inconsistente

Serão apresentadas nesta seção apenas as diferenças em relação aos esquemas da seção anterior.

2.3.1 Contorno norte

1. Aproximações

O termo envolvendo a derivada em relação a ξ é desprezada na condição de contorno

$$-\beta_s \left(\frac{\partial \phi}{\partial \xi} \right)_s + \gamma_s \left(\frac{\partial \phi}{\partial \eta} \right)_s = 0, \quad \phi \in \{p, T\}, \quad (69)$$

de modo que resta

$$\left(\frac{\partial \phi}{\partial \eta} \right)_s = \frac{\phi_P - \phi_S}{\Delta \eta} = 0. \quad (70)$$

2. Extrapolações para os fictícios

Com base nas aproximações apresentadas acima, tem-se

$$T_P = T_S \quad (71)$$

$$p_P = p_S \quad (72)$$

3. Coeficientes dos sistemas lineares

Com base nas aproximações apresentadas acima, tem-se

$$A_P^T = 1, \quad A_S^T = -1, \quad b_P^T = 0 \quad (73)$$

e

$$A_P^{p'} = 1, \quad A_S^{p'} = -1, \quad b_P^{p'} = 0. \quad (74)$$

2.3.2 Contorno leste

1. Aproximações

Na condição de contorno

$$U_w \left(\frac{\partial \phi}{\partial \xi} \right)_w + V_w \left(\frac{\partial \phi}{\partial \eta} \right)_w, \quad \phi \in \{p, T, u, v\}. \quad (75)$$

o termo envolvendo V_w é desprezado, de modo que

$$\frac{\partial \phi}{\partial \xi} = \frac{\phi_P - \phi_W}{\Delta \xi} = 0, \quad \phi \in \{p, T, u, v\}. \quad (76)$$

2. Extrapolações para os fictícios

Com base nas aproximações acima, tem-se

$$\phi_P = \phi_W, \quad \phi \in \{u, v, T, p\}. \quad (77)$$

3. Coeficientes dos sistemas lineares

Com base nas aproximações acima, tem-se

$$A_P^\phi = 1, \quad A_W^\phi = -1, \quad b_P^\phi = 0, \quad \phi \in \{u, v, T, p'\}. \quad (78)$$

3 Comparações

Para comparar os resultados do código que não utiliza o esquema consistente com o que utiliza, foram realizados dois conjuntos de simulações. O conjunto S0123 utiliza o código com condições de contorno inconsistentes, enquanto o conjunto S0124 utiliza o código com condições de contorno consistentes. Os parâmetros de entrada de ambos os códigos são mostrados na Tab. 1, que também apresenta os parâmetros comuns a todas as simulações.

3.1 Parâmetros numéricos

Tabela 1: Parâmetros numéricos de entrada

| | | |
|---|-----------|------------|
| Simulation identification (up to 100 characters) | sim_id | |
| Number of real volumes in the csi direction | nx2 | |
| Number of real volumes in the eta direction | ny2 | |
| Kind of grid (1=eta uniform, 2=geometric progression for eta, 3=power law) | kg | 1 |
| Initial step for the geometric progression grid (m) | a1 | 1.d-6 |
| Coordinate system (1=cylindrical, else cartesian) | coord | 1 |
| Perfect gas constant (J/(kg.K)) | Rg | 2.869E+02 |
| gamma = Cpo / Cvo in the chamber (Specific heat ratio) | gamma | 1.4d0 |
| Stagnation pressure in the chamber (Pa) | po | 1725068.d0 |
| Stagnation temperature in the chamber (K) | T0 | 833.33d0 |
| atmospheric pressure at the sea level (Pa) | pr | 101325 |
| gravitational acceleration at the sea level (m/s2) | go | 9.80665d0 |
| Initial constant of the UDS/CDS mixing scheme | beta1 | 0.0d0 |
| Final constant of the UDS/CDS mixing scheme | beta2 | 0.0d0 |
| beta = beta1 for it <= itb1 | itb1 | 1000 |
| beta = beta2 for itb2 <= it | itb2 | 1000 |
| modvis = 0 -> Euler; modvis = 1 -> Navier-Stokes | modvis | 0 |
| turbulence model option (0=laminar, 1=Baldwin-Lomax) | modtur | 0 |
| ccTw = 0 -> adiabatic; ccTw = 1 -> prescribed temperature | ccTw | 0 |
| dt = dt1 for it <= it1 | it1 | 5 |
| dt = dt2 for it2 <= it | it2 | 5 |
| Initial time step (s) | dt1 | |
| Final time step (s) | dt2 | |
| Maximum number of iterations of the time evolution | itmax | |
| Parada com base no valor do resiuo, se negativo, a parada eh feita com base no imax | tolerance | -1d-13 |
| Maximum number of iterations for the pressure correction | imax | 5 |
| Maximum number of iterations for the TDMA method for u, v and T | nitm_u | 2 |
| Maximum number of iterations for the TDMA method for p | nitm_p | 2 |
| Upload backup data and continue computation (0 = no, 1 = yes) | reload | 0 |
| Frequency of saving backup data | wbcp | 50000 |
| Frequency of printing in the listing file and in the screen | wlf | 1 |
| 1 = do not open result files, 0 = open | sem_a | 1 |
| 0 = visualize the plot, 1 = do not visualize | sem_g | 1 |
| Frequency of writing data for graphics | w_g | 1 |
| 1 = write the fields, 0 = do not | w_cam | 1 |
| Mostrar resultados de iteracoes na tela, 0 = nao, 1= sim | ver_tela | 0 |
| N. de Nucleos que serao utilizados na comp. paralela | num | 1 |

3.2 Cd e Fd*

A Tab. 2 apresenta os resultados dos conjuntos S0123 e S0124. As quatro últimas linhas desta tabela mostram as diferenças relativas de Cd e Fd*.

Tabela 2: Comparação de Cd e Fd* dos conjuntos de simulações S0123 e S0124.

| S0123 | | | | | | | | | |
|------------|-----|-----|-------|----------|---------|---------|-----------------------|-----------------------|-------|
| Simulation | nx | ny | itmax | tcpu | dt1 | dt2 | Cd | | Fd* |
| S01 | 58 | 22 | 2000 | 2.487 | 5.0E+00 | 5.0E+00 | 1.047087004682598E+00 | 9.718063318656711E-01 | 0.35% |
| S02 | 114 | 42 | 4000 | 21.45 | 5.0E+00 | 5.0E+00 | 1.016956161749266E+00 | 9.698146418197395E-01 | 0.10% |
| S03 | 226 | 82 | 16000 | 439.496 | 5.0E+00 | 5.0E+00 | 1.000836328728608E+00 | 9.691914048072179E-01 | 0.03% |
| S04 | 450 | 162 | 45000 | 8140.022 | 5.0E+00 | 5.0E+00 | 9.914742089823384E-01 | 9.681901799767691E-01 | 0.01% |
| S0124 | | | | | | | | | |
| Simulation | nx | ny | itmax | tcpu | dt1 | dt2 | Cd | | Fd* |
| S01 | 58 | 22 | 2000 | 2.643 | 5.0E+00 | 5.0E+00 | 1.043961624320509E+00 | 9.683953205124902E-01 | 0.35% |
| S02 | 114 | 42 | 4000 | 23.339 | 5.0E+00 | 5.0E+00 | 1.016084463106510E+00 | 9.687987924374382E-01 | 0.10% |
| S03 | 226 | 82 | 16000 | 457.851 | 5.0E+00 | 5.0E+00 | 1.000647467320118E+00 | 9.689439710818043E-01 | 0.03% |
| S04 | 450 | 162 | 45000 | 8127.345 | 5.0E+00 | 5.0E+00 | 9.914315208637893E-01 | 9.681289058145962E-01 | 0.01% |

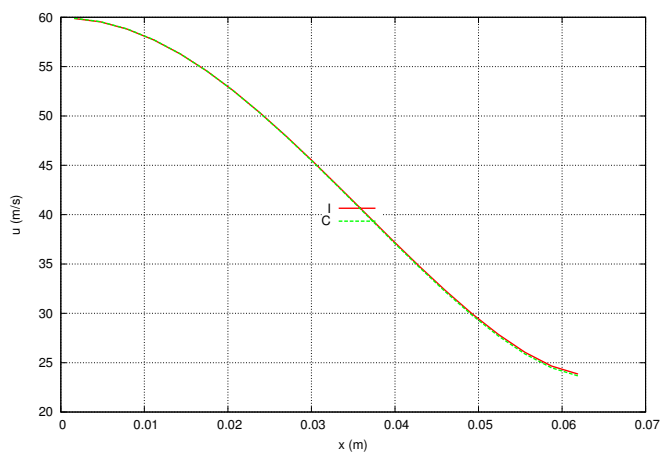
3.3 Campos u , v , T e p

3.3.1 Malha 56×20

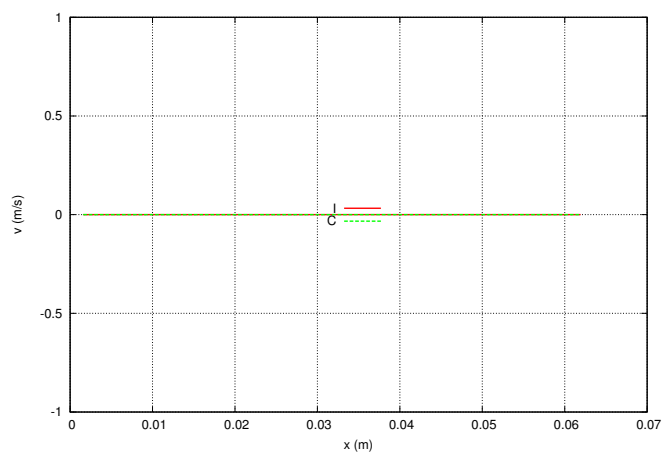
A tabela a seguir mostra a diferença relativa entre as soluções com condição de contorno inconsistente (S0123) e consistente (S0124).

Max. relative difference

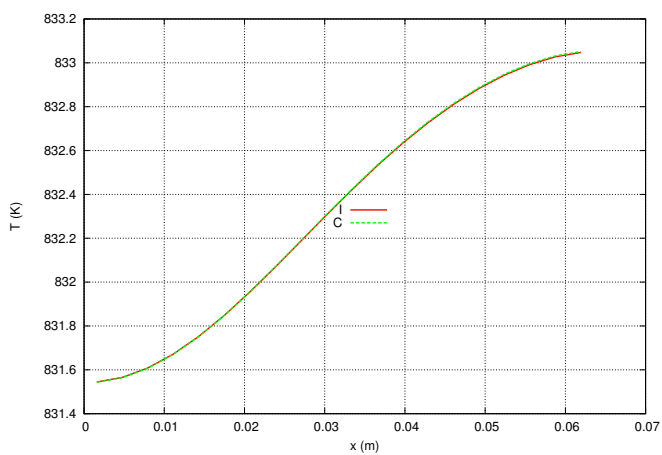
| Var. | Node | South | North | West | East |
|------|-----------|-----------|-----------|-----------|-----------|
| u | 1.007E-01 | 1.907E-03 | 7.051E-02 | 7.705E-03 | 9.638E-03 |
| v | 1.409E+00 | 0.000E+00 | 7.051E-02 | Infinity | 3.014E-02 |
| T | 1.692E-02 | 8.298E-04 | 1.654E-02 | 5.326E-06 | 1.282E-02 |
| p | 1.983E-02 | 3.317E-03 | 1.878E-02 | 1.866E-05 | 7.962E-03 |



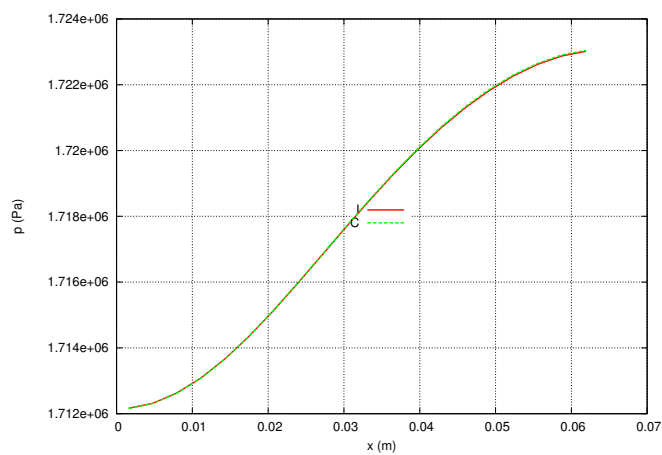
(a) u



(b) v

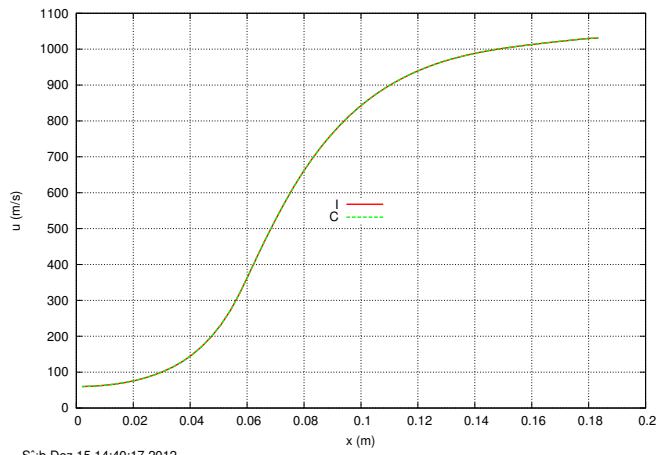


(c) T



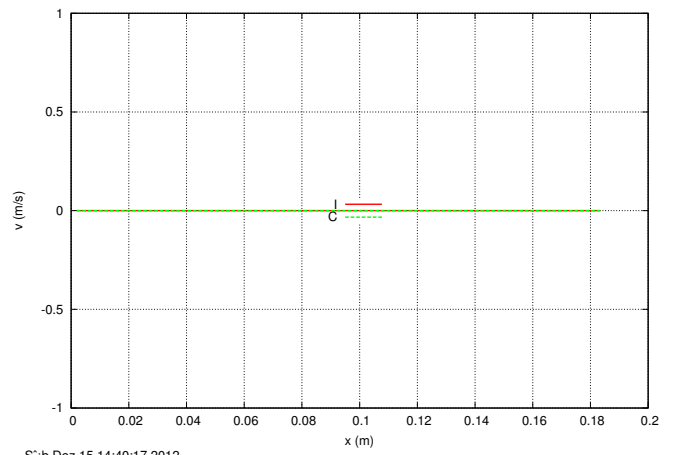
(d) p

Figura 2: Comparação dos campos de velocidade, temperatura e pressão no contorno oeste utilizando o esquema numérico consistente (C) e inconsistente (I) na malha 56×20 .



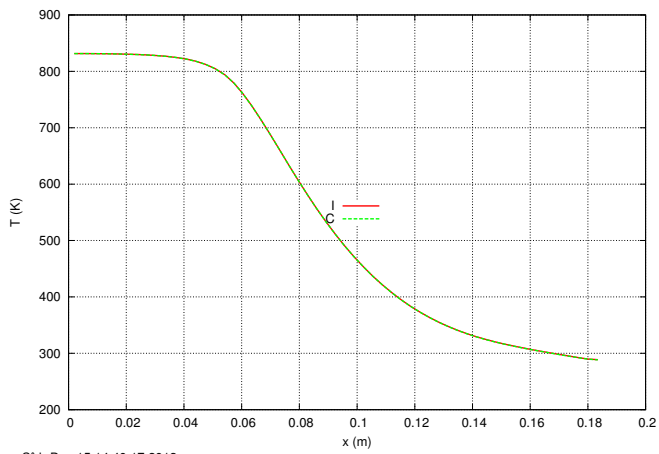
S:\b Dez 15 14:40:17 2012

(a) u



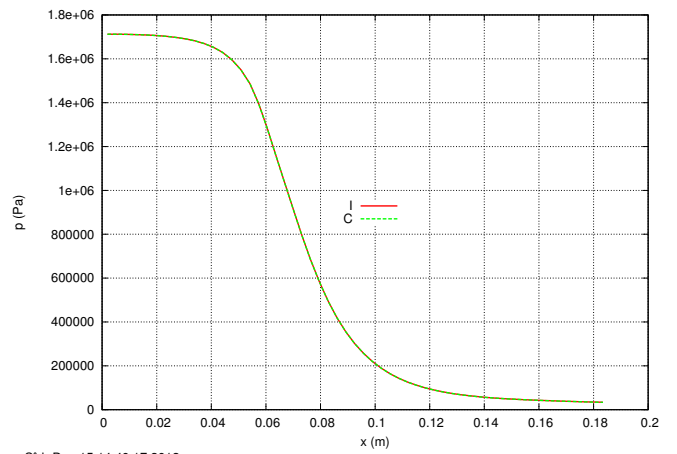
S:\b Dez 15 14:40:17 2012

(b) v



S:\b Dez 15 14:40:17 2012

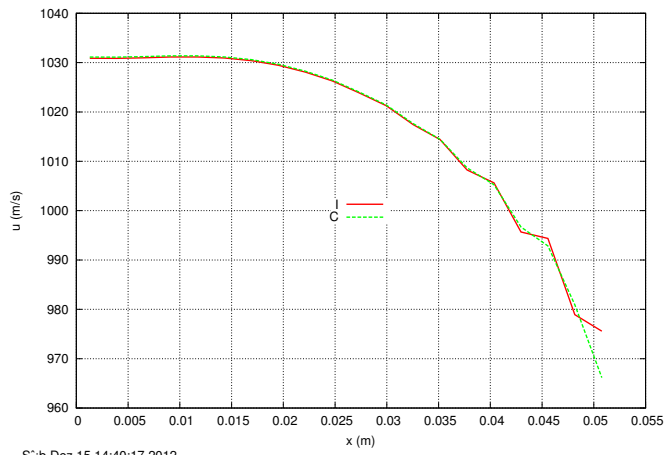
(c) T



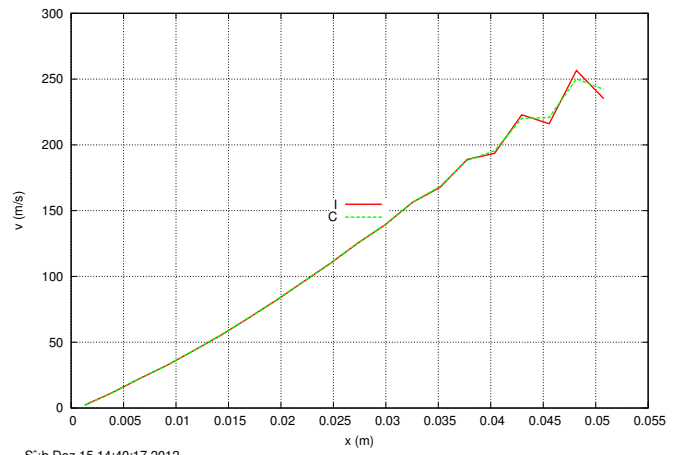
S:\b Dez 15 14:40:17 2012

(d) p

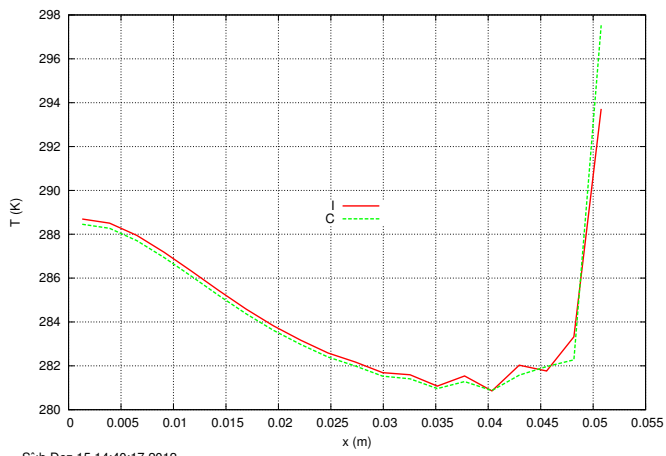
Figura 3: Comparação dos campos de velocidade, temperatura e pressão no contorno sul utilizando o esquema numérico consistente (C) e inconsistente (I) na malha 56×20 .



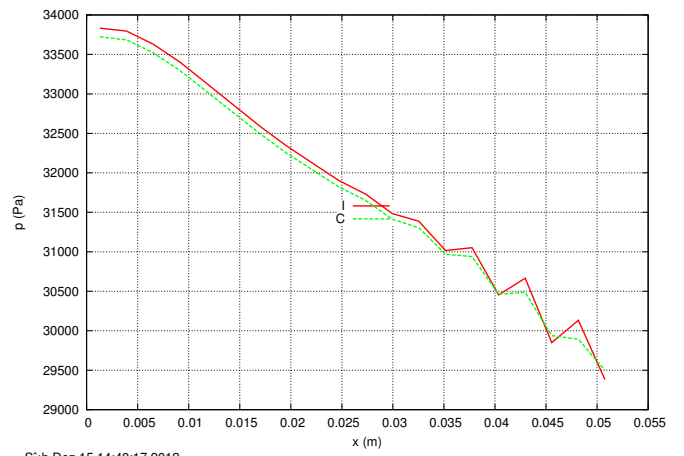
(a) u



(b) v

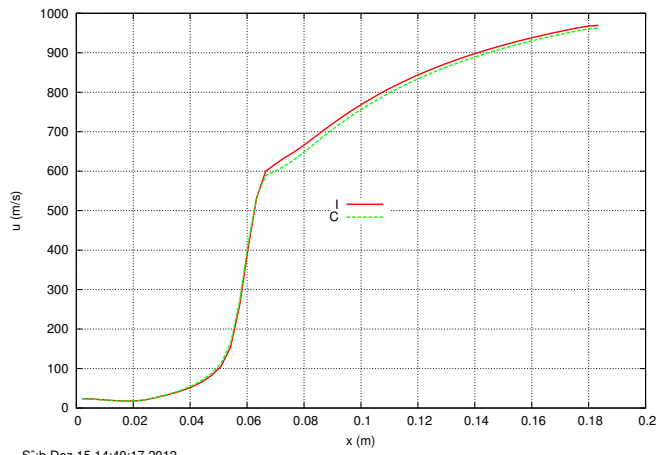


(c) T

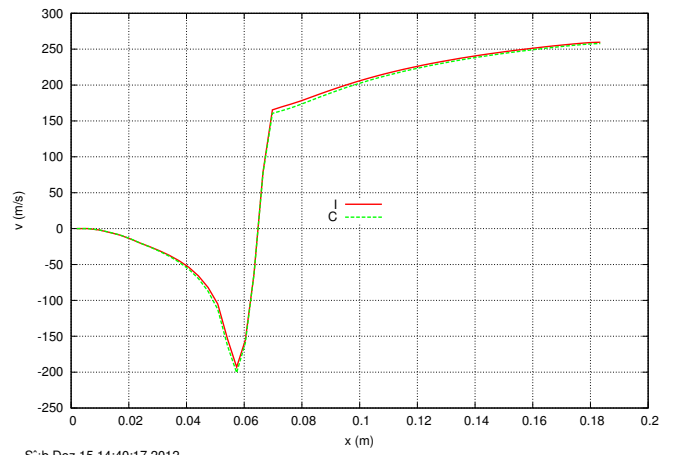


(d) p

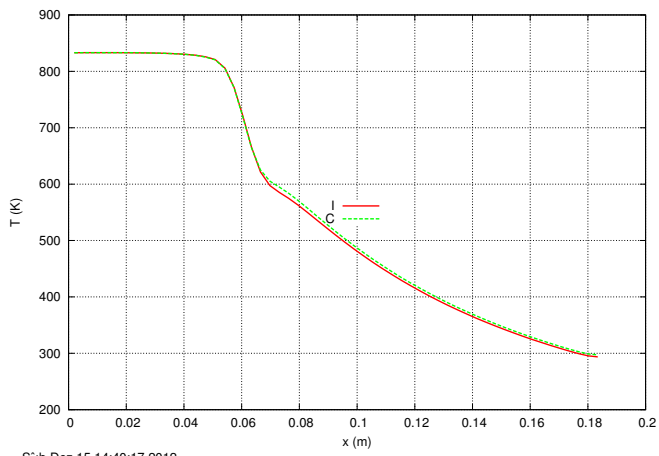
Figura 4: Comparação dos campos de velocidade, temperatura e pressão no contorno leste utilizando o esquema numérico consistente (C) e inconsistente (I) na malha 56×20 .



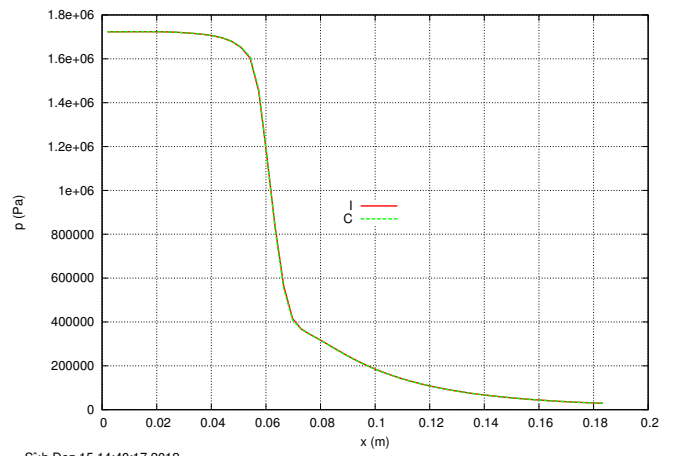
(a) u



(b) v



(c) T



(d) p

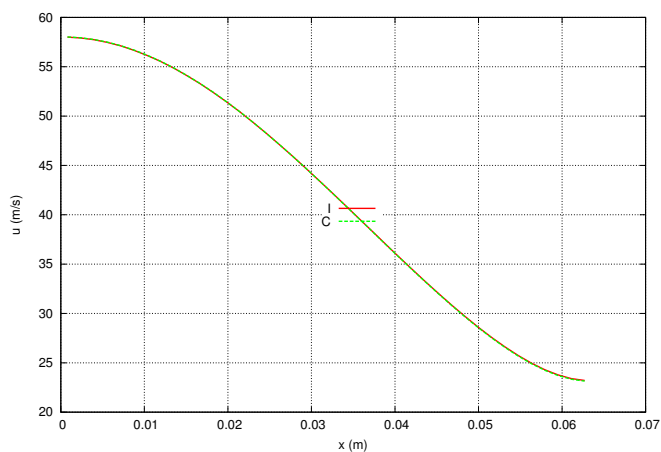
Figura 5: Comparação dos campos de velocidade, temperatura e pressão no contorno norte utilizando o esquema numérico consistente (C) e inconsistente (I) na malha 56×20 .

3.3.2 Malha 112×40

A tabela a seguir mostra a diferença relativa entre as soluções com condição de contorno inconsistente (S0123) e consistente (S0124).

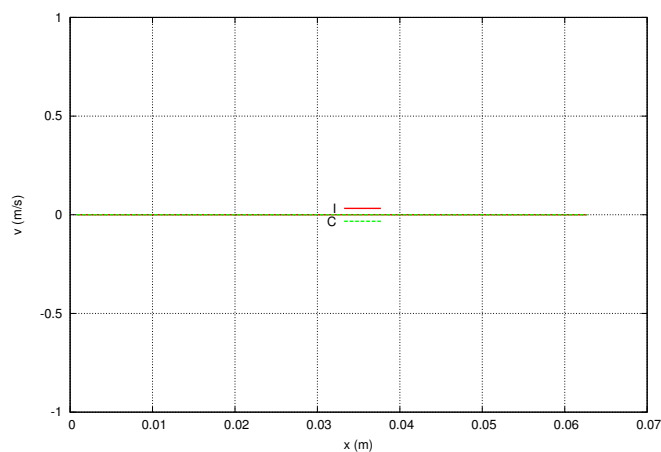
Max. relative difference

| Var. | Node | South | North | West | East |
|------|-----------|-----------|-----------|-----------|-----------|
| u | 9.174E-02 | 1.171E-03 | 6.131E-02 | 2.679E-03 | 6.697E-03 |
| v | 1.669E+00 | 0.000E+00 | 6.131E-02 | Infinity | 1.870E-02 |
| T | 1.670E-02 | 5.185E-04 | 1.664E-02 | 1.728E-06 | 1.167E-02 |
| p | 1.271E-02 | 1.746E-03 | 8.956E-03 | 6.045E-06 | 3.479E-03 |



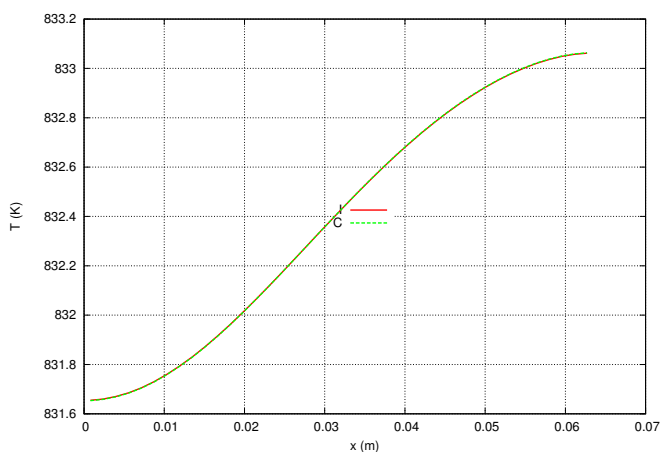
S\|b Dez 15 14:50:28 2012

(a) u



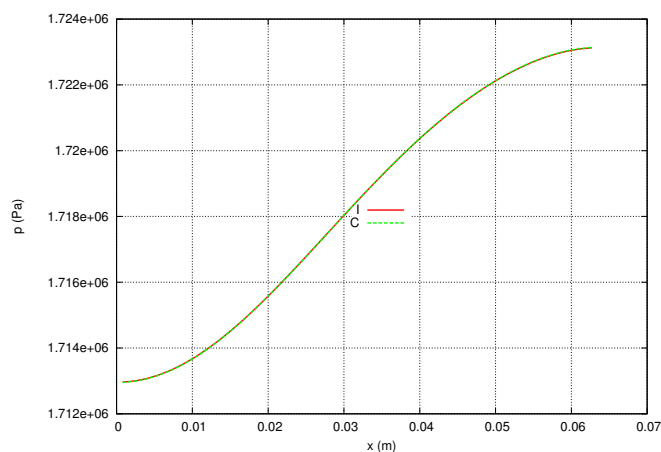
S\|b Dez 15 14:50:28 2012

(b) v



S\|b Dez 15 14:50:28 2012

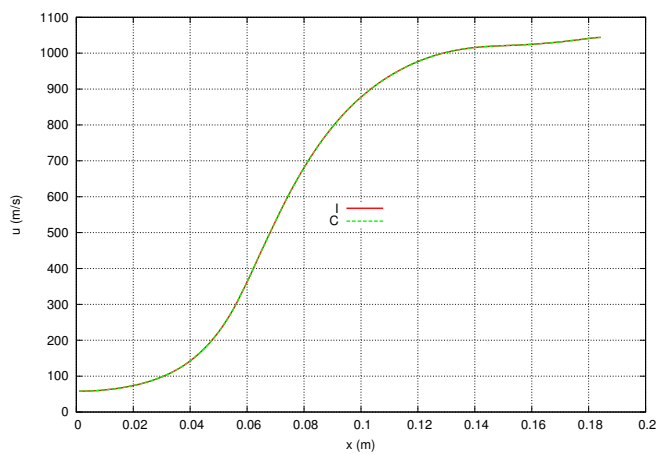
(c) T



S\|b Dez 15 14:50:28 2012

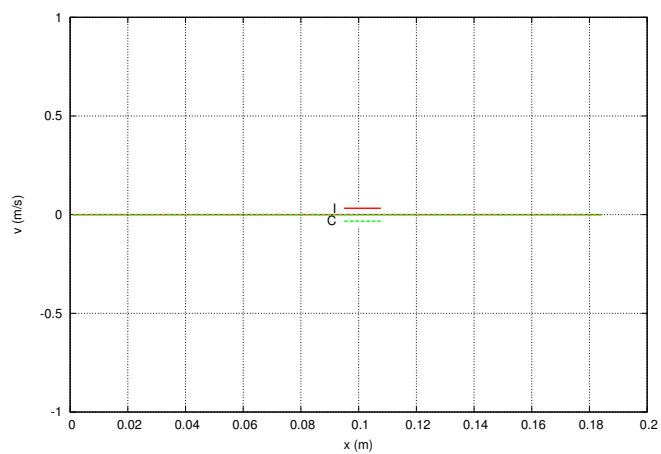
(d) p

Figura 6: Comparação dos campos de velocidade, temperatura e pressão no contorno oeste utilizando o esquema numérico consistente (C) e inconsistente (I) na malha 112×40 .



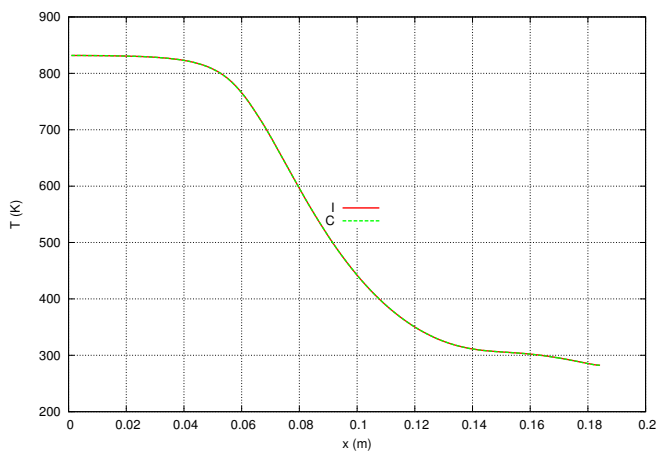
S:\b Dez 15 14:50:28 2012

(a) u



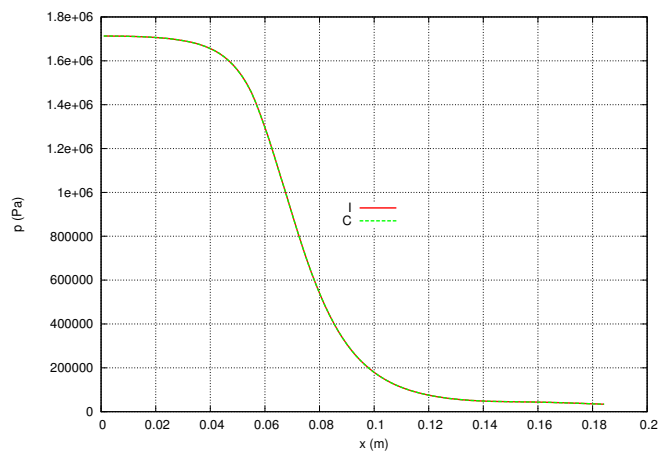
S:\b Dez 15 14:50:28 2012

(b) v



S:\b Dez 15 14:50:28 2012

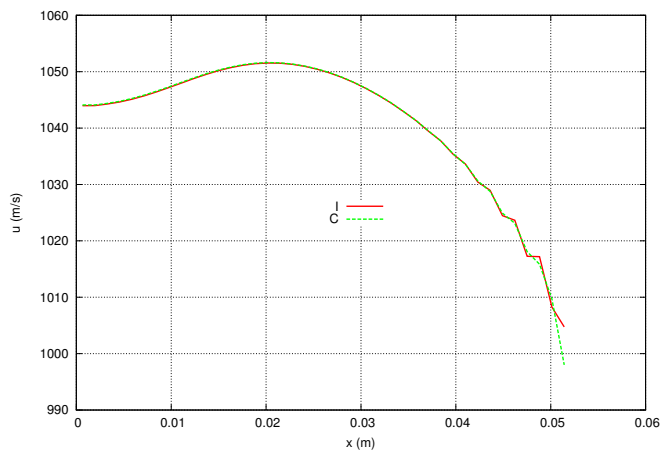
(c) T



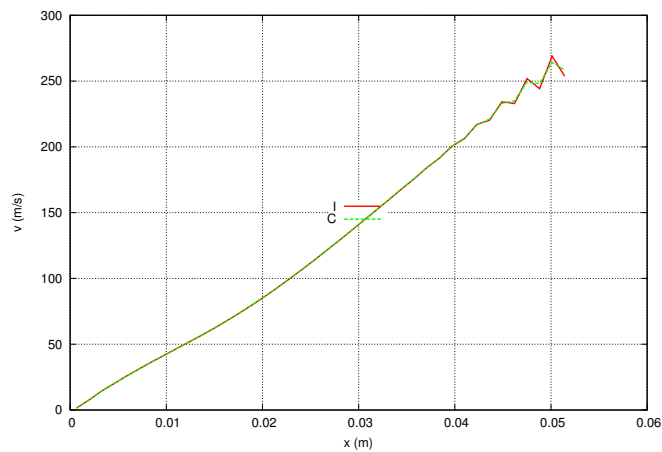
S:\b Dez 15 14:50:28 2012

(d) p

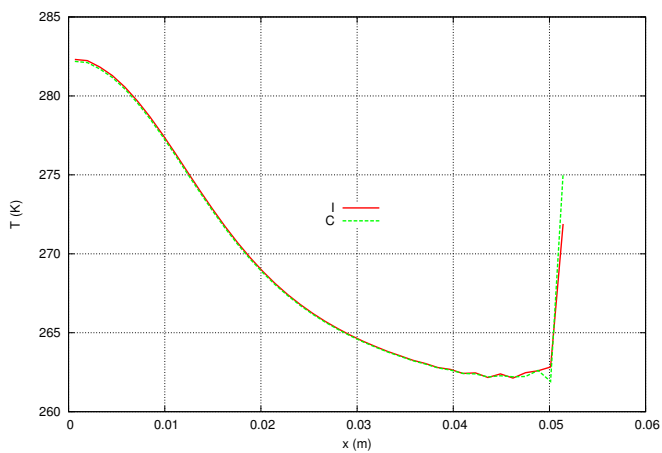
Figura 7: Comparação dos campos de velocidade, temperatura e pressão no contorno sul utilizando o esquema numérico consistente (C) e inconsistente (I) na malha 112×40 .



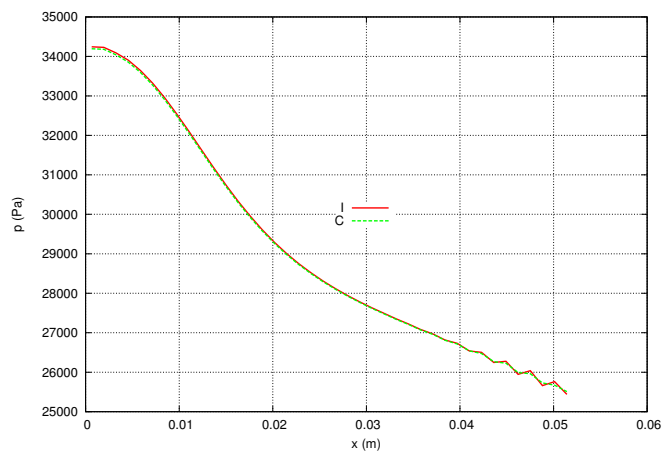
(a) u



(b) v

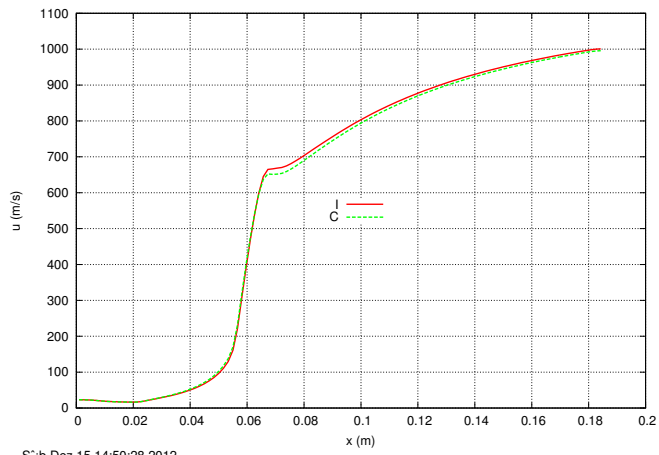


(c) T

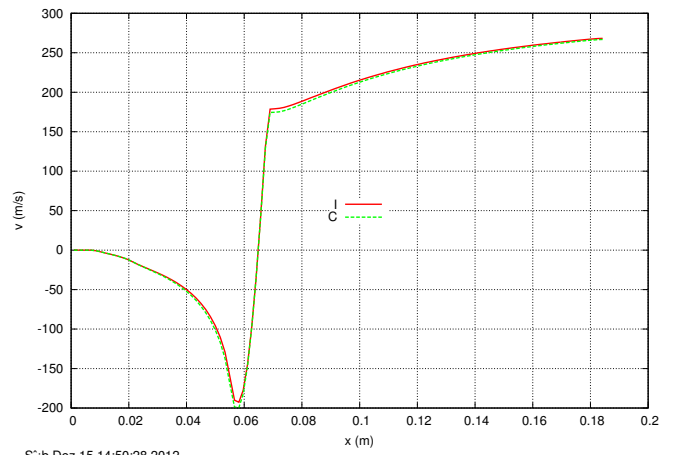


(d) p

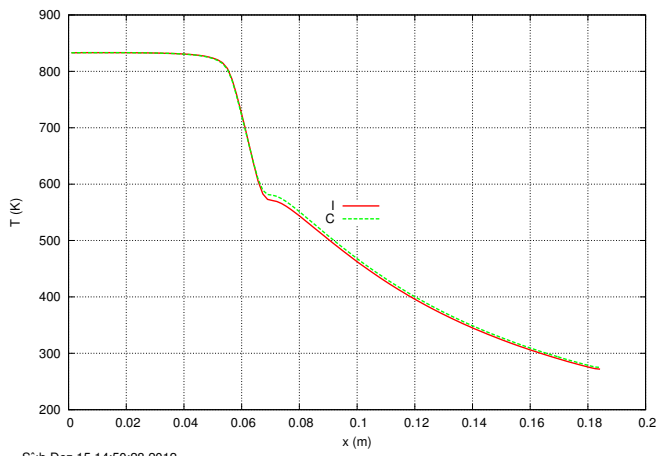
Figura 8: Comparação dos campos de velocidade, temperatura e pressão no contorno leste utilizando o esquema numérico consistente (C) e inconsistente (I) na malha 112×40 .



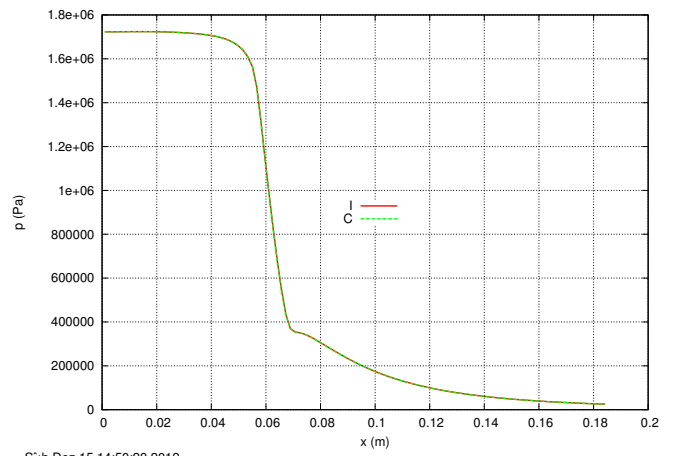
(a) u



(b) v



(c) T



(d) p

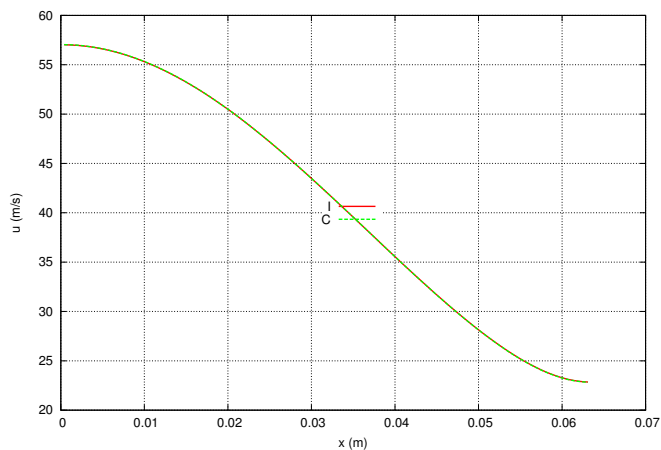
Figura 9: Comparação dos campos de velocidade, temperatura e pressão no contorno norte utilizando o esquema numérico consistente (C) e inconsistente (I) na malha 112×40 .

3.3.3 Malha 224×80

A tabela a seguir mostra a diferença relativa entre as soluções com condição de contorno inconsistente (S0123) e consistente (S0124).

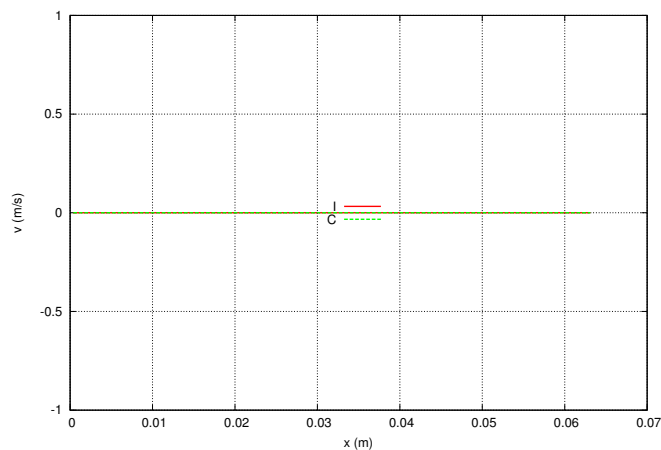
Max. relative difference

| Var. | Node | South | North | West | East |
|------|-----------|-----------|-----------|-----------|-----------|
| u | 8.062E-02 | 5.873E-04 | 5.107E-02 | 8.562E-04 | 4.114E-03 |
| v | 1.366E+01 | 0.000E+00 | 5.107E-02 | Infinity | 1.287E-02 |
| T | 1.351E-02 | 2.698E-04 | 1.354E-02 | 1.094E-06 | 8.517E-03 |
| p | 6.443E-03 | 8.869E-04 | 3.876E-03 | 3.826E-06 | 1.713E-03 |



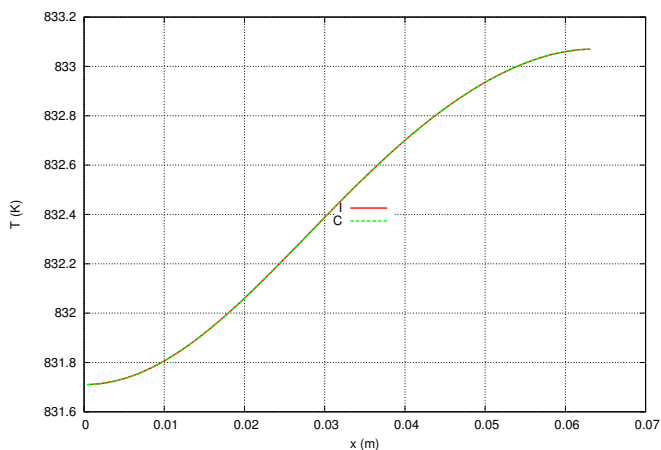
S:\b Dez 15 14:50:31 2012

(a) u



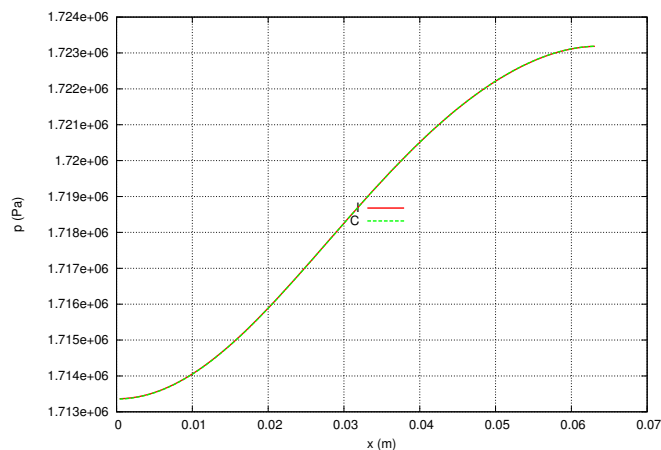
S:\b Dez 15 14:50:31 2012

(b) v



S:\b Dez 15 14:50:31 2012

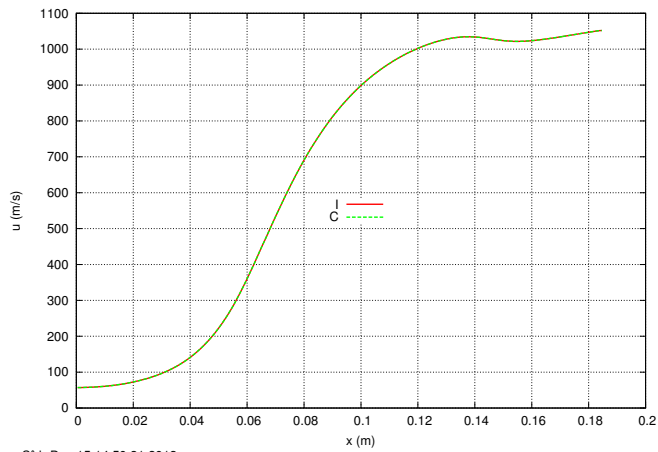
(c) T



S:\b Dez 15 14:50:31 2012

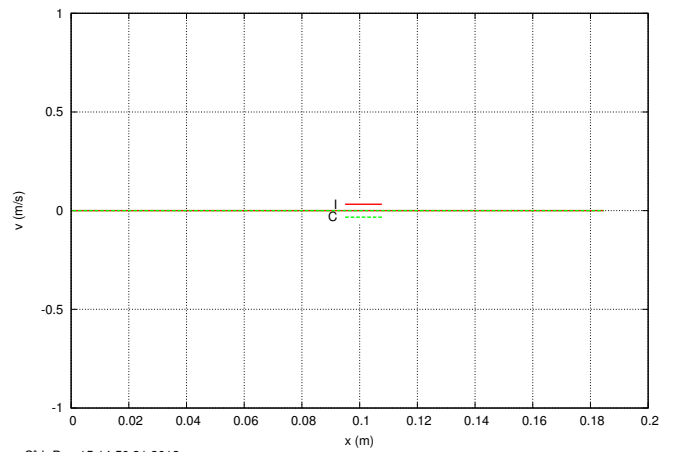
(d) p

Figura 10: Comparação dos campos de velocidade, temperatura e pressão no contorno oeste utilizando o esquema numérico consistente (C) e inconsistente (I) na malha 224×80 .



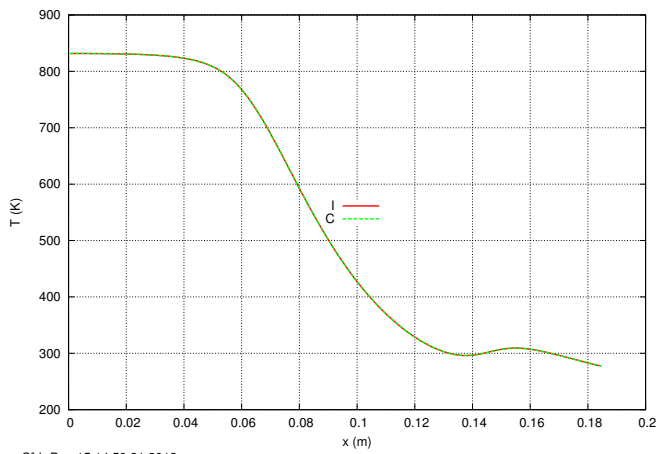
S:\b Dez 15 14:50:31 2012

(a) u



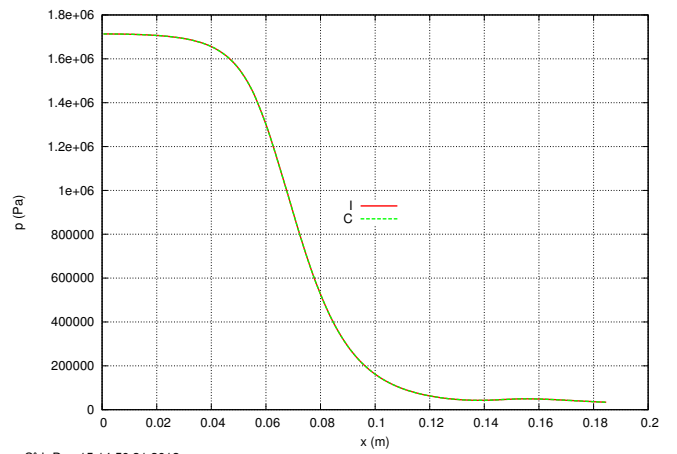
S:\b Dez 15 14:50:31 2012

(b) v



S:\b Dez 15 14:50:31 2012

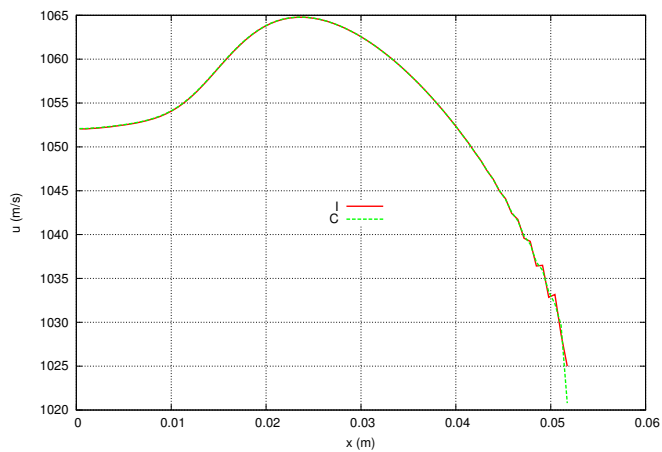
(c) T



S:\b Dez 15 14:50:31 2012

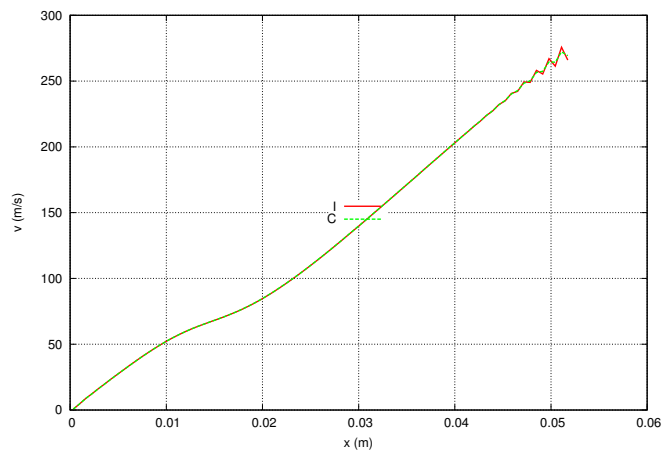
(d) p

Figura 11: Comparação dos campos de velocidade, temperatura e pressão no contorno sul utilizando o esquema numérico consistente (C) e inconsistente (I) na malha 224×80 .



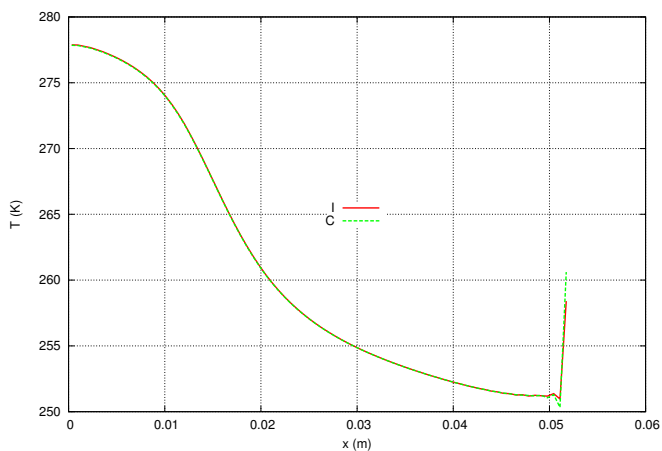
Sáb Dez 15 14:50:31 2012

(a) u



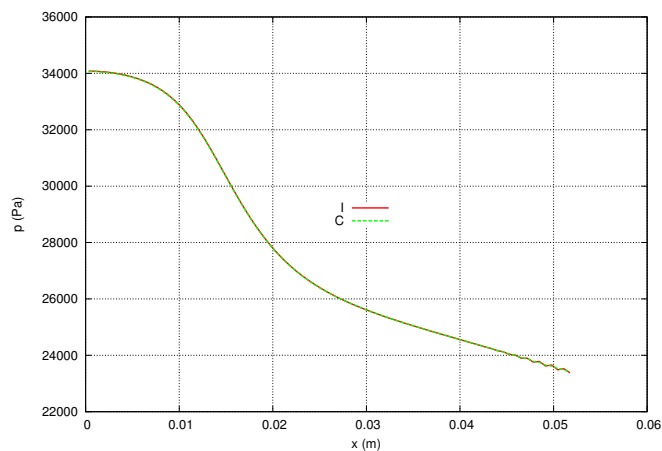
Sáb Dez 15 14:50:31 2012

(b) v



Sáb Dez 15 14:50:31 2012

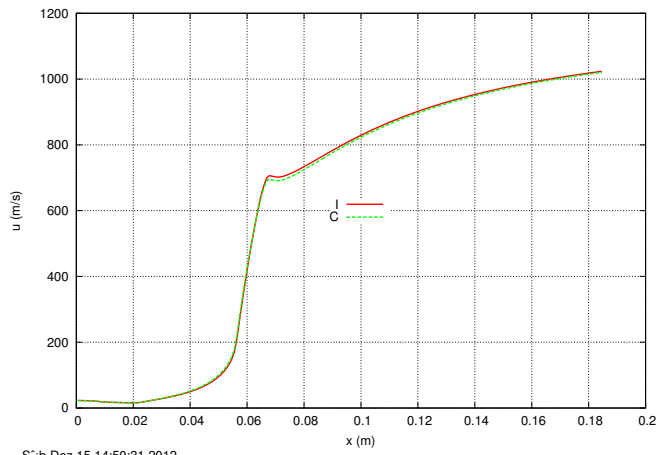
(c) T



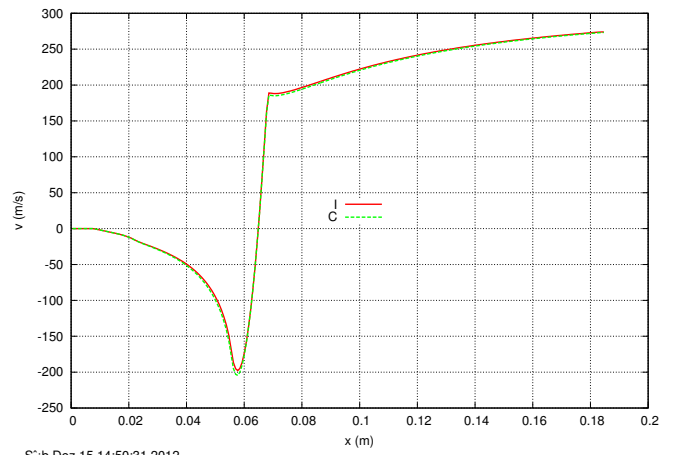
Sáb Dez 15 14:50:31 2012

(d) p

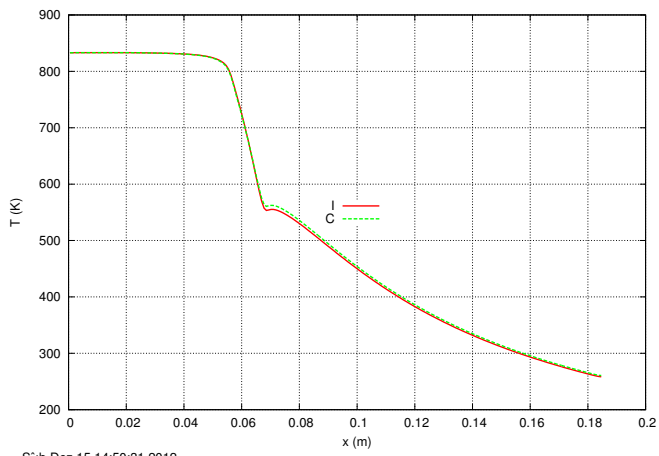
Figura 12: Comparação dos campos de velocidade, temperatura e pressão no contorno leste utilizando o esquema numérico consistente (C) e inconsistente (I) na malha 224×80 .



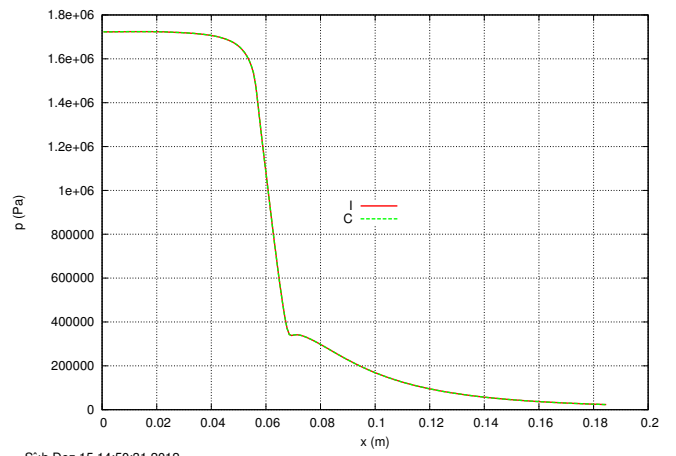
(a) u



(b) v



(c) T



(d) p

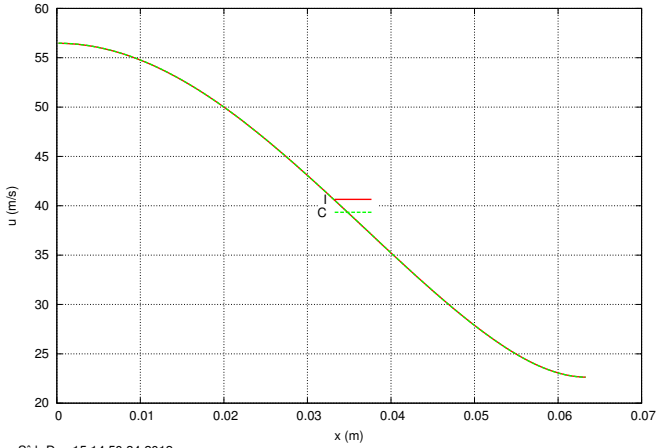
Figura 13: Comparação dos campos de velocidade, temperatura e pressão no contorno norte utilizando o esquema numérico consistente (C) e inconsistente (I) na malha 224×80 .

3.3.4 Malha 448×160

A tabela a seguir mostra a diferença relativa entre as soluções com condição de contorno inconsistente (S0123) e consistente (S0124).

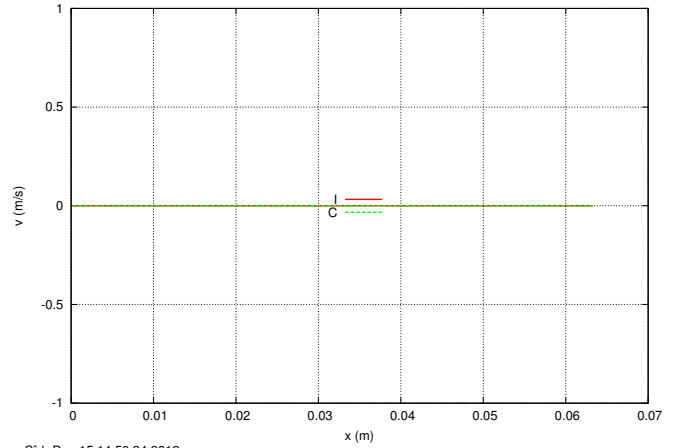
Max. relative difference

| Var. | Node | South | North | West | East |
|------|-----------|-----------|-----------|-----------|-----------|
| u | 6.831E-02 | 2.333E-04 | 4.113E-02 | 2.817E-04 | 2.279E-03 |
| v | 1.835E+03 | 0.000E+00 | 4.113E-02 | Infinity | 8.694E-03 |
| T | 9.271E-03 | 1.484E-04 | 9.270E-03 | 4.732E-07 | 5.277E-03 |
| p | 3.239E-03 | 5.307E-04 | 1.927E-03 | 1.656E-06 | 8.832E-04 |



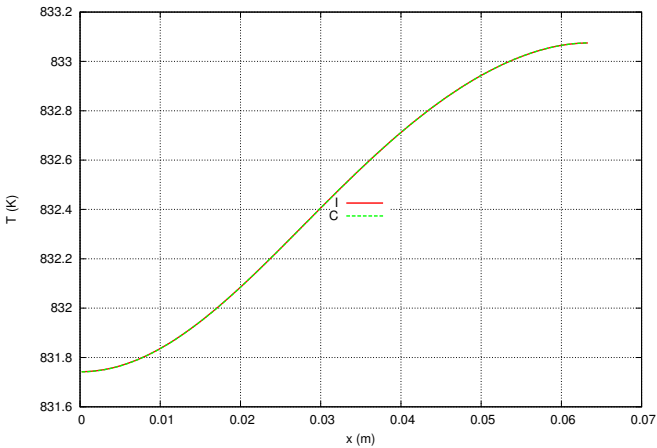
S:\b Dez 15 14:50:34 2012

(a) u



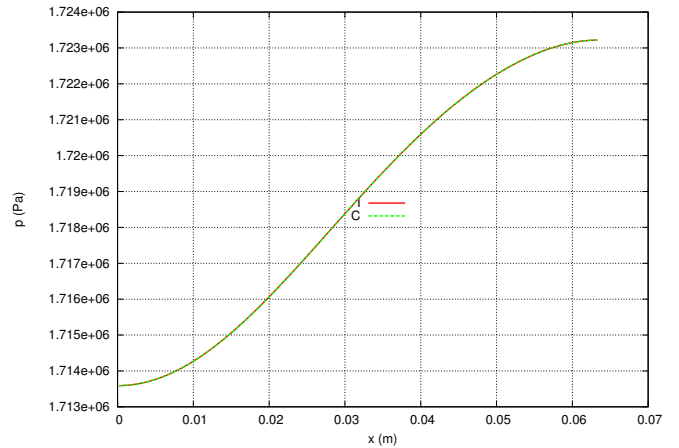
S:\b Dez 15 14:50:34 2012

(b) v



S:\b Dez 15 14:50:34 2012

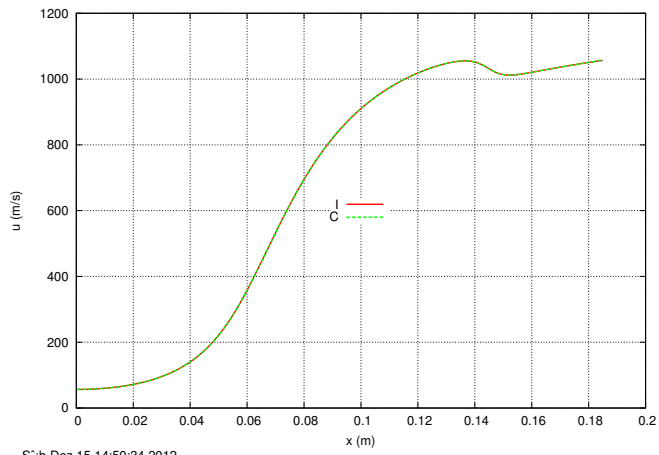
(c) T



S:\b Dez 15 14:50:34 2012

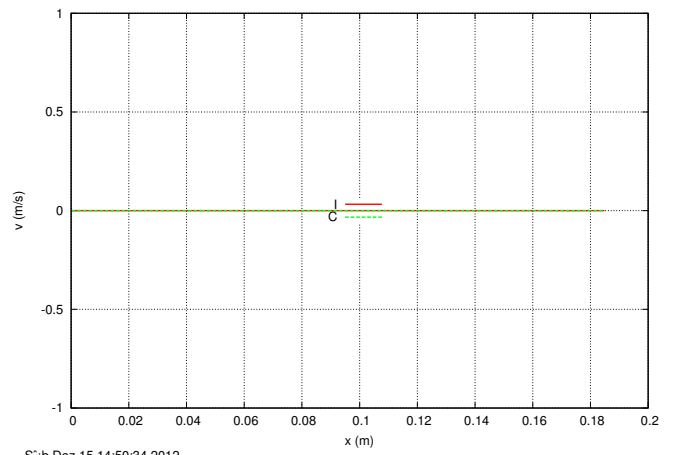
(d) p

Figura 14: Comparação dos campos de velocidade, temperatura e pressão no contorno oeste utilizando o esquema numérico consistente (C) e inconsistente (I) na malha 448×160 .



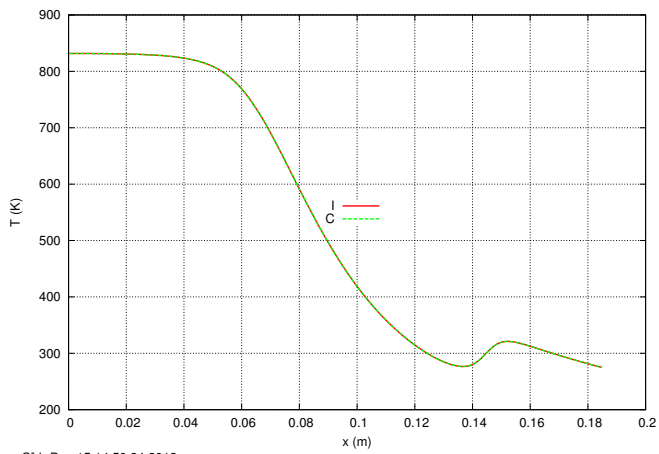
S:\b Dez 15 14:50:34 2012

(a) u



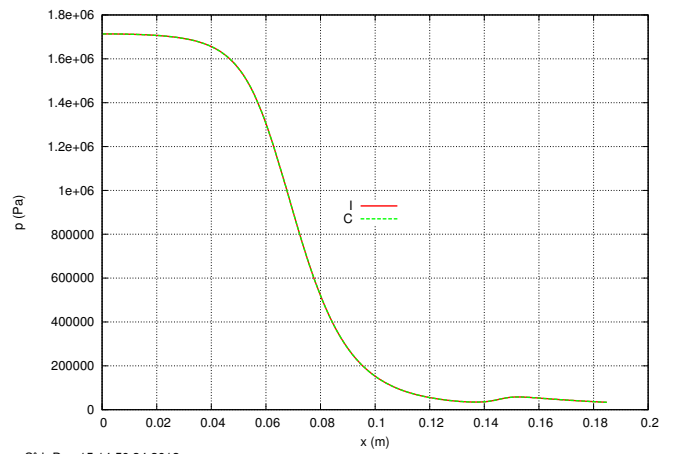
S:\b Dez 15 14:50:34 2012

(b) v



S:\b Dez 15 14:50:34 2012

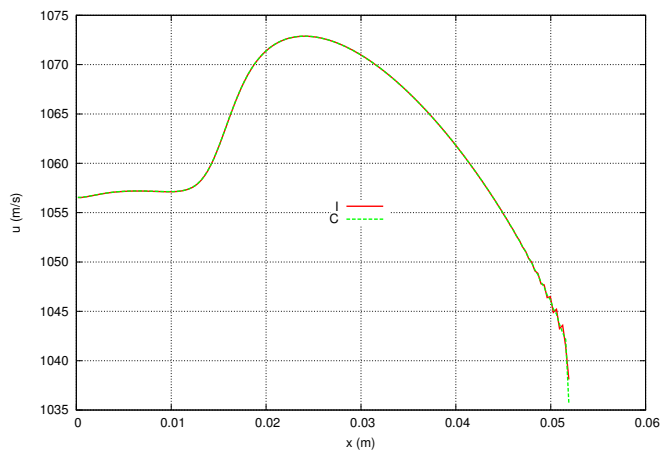
(c) T



S:\b Dez 15 14:50:34 2012

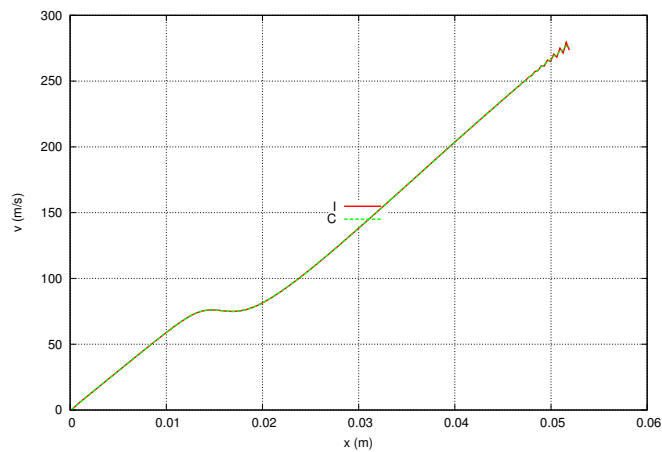
(d) p

Figura 15: Comparação dos campos de velocidade, temperatura e pressão no contorno sul utilizando o esquema numérico consistente (C) e inconsistente (I) na malha 448×160 .



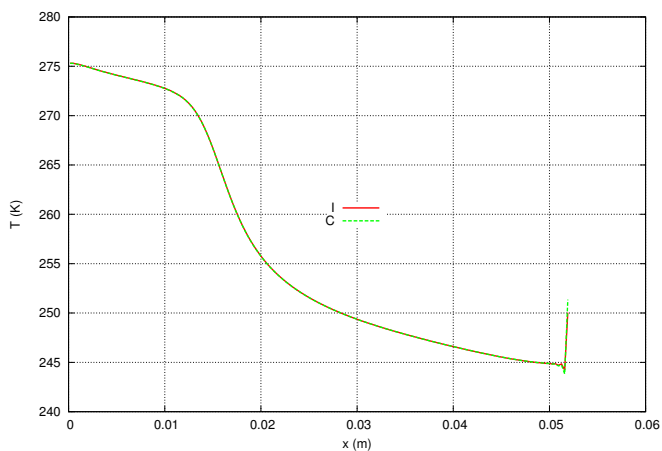
S:\b Dez 15 14:50:34 2012

(a) u



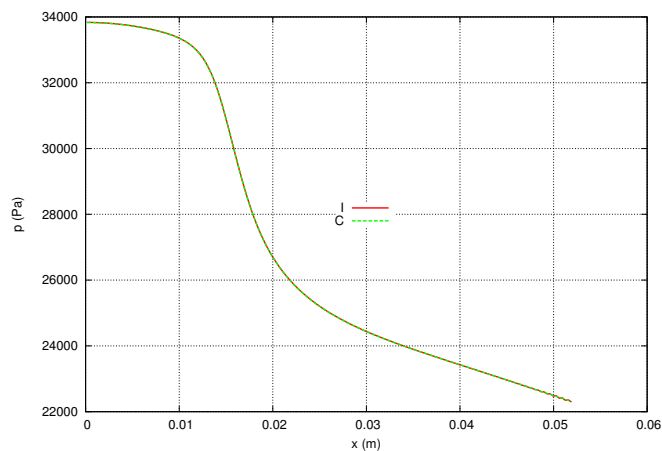
S:\b Dez 15 14:50:34 2012

(b) v



S:\b Dez 15 14:50:34 2012

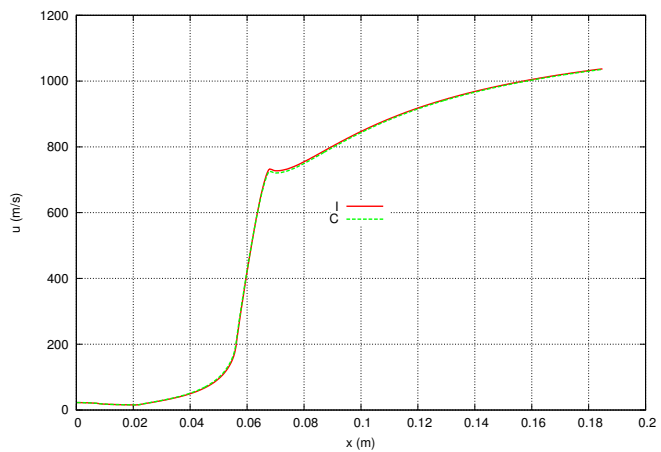
(c) T



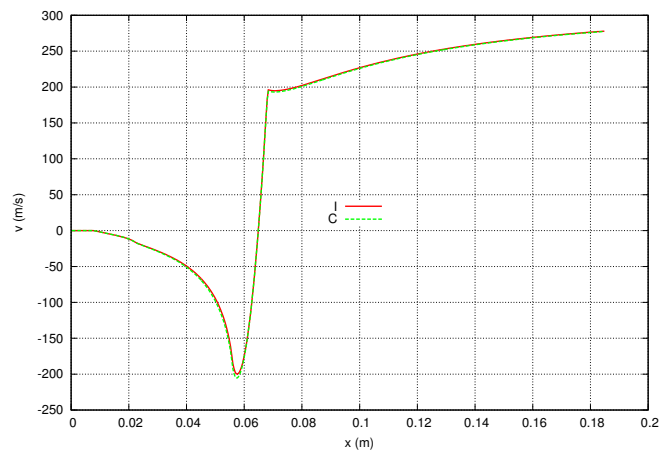
S:\b Dez 15 14:50:34 2012

(d) p

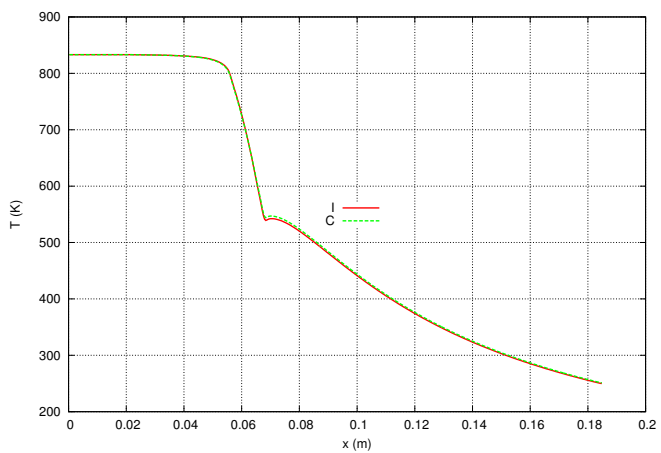
Figura 16: Comparação dos campos de velocidade, temperatura e pressão no contorno leste utilizando o esquema numérico consistente (C) e inconsistente (I) na malha 448×160 .



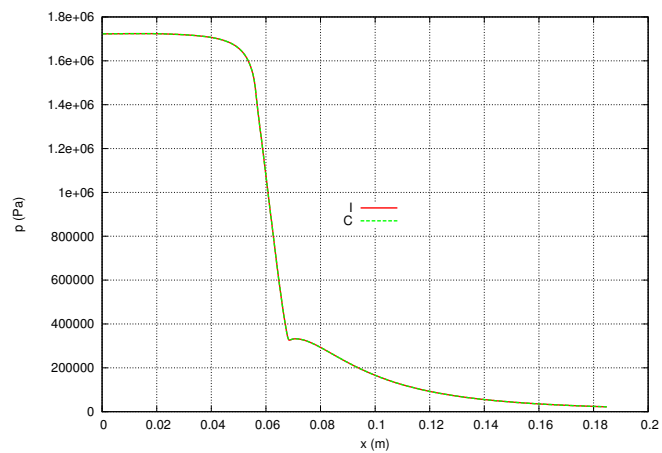
(a) u



(b) v



(c) T



(d) p

Figura 17: Comparação dos campos de velocidade, temperatura e pressão no contorno norte utilizando o esquema numérico consistente (C) e inconsistente (I) na malha 448×160 .

3.3.5 Panorama geral

A Tab. 3 mostra como a máxima diferença relativa entre os campos obtidos com os esquemas consistente e inconsistente varia com o refino da malha.

Tabela 3: Máxima diferença relativa dos campos com o refino da malha.

| malha | u | v | T | p |
|---------|--------|------|-------|-------|
| 56x20 | 10.07% | Inf. | 1.69% | 1.98% |
| 112x40 | 9.17% | Inf. | 1.67% | 1.27% |
| 224x80 | 8.06% | Inf. | 1.35% | 0.64% |
| 448x160 | 6.83% | Inf. | 0.93% | 0.32% |

4 Conclusões

Ao se comparar os resultados obtidos com os esquemas numéricos consistente e inconsistentes nas condições de contorno, chegou-se às seguintes conclusões

1. As variáveis Cd e Fd^* são afetadas pela mudança de esquema, mas a diferença relativa dos resultados diminui com o refino da malha. Na malha mais grossa (56x20) a diferença relativa foi de 0,35% e na malha mais fina (448x160) foi da ordem de 0,01%.
2. Os campos u , v , T e p também são afetados pela mudança de esquema. Dentre eles, o que teve maior variação relativa foi v , seguido por u , T e p . As variações elevadas em v se justificam pelo fato desta variável ser nula ou próxima de zero em alguns pontos do domínio. Na malha mais fina (448x160), as máximas diferenças relativas foram 7% para u , 1% para T e 0,3% para p .

A Revisões do código Mach2D-7-SVN-r201

Branch CBC (Consistent boundary conditions)

Parent: tag Diego_version_for_linux; SVN-r91

In this branch will be implemented a consistent scheme for the boundary conditions.
A consistent scheme is the one that reduces to the exact BC as the mesh is refined.

r187

====

File comments.txt added.

r188

====

Added the subroutine 'get_mass_conservation_check' that calculates the norm L_{inf} of the res. of the mass conservation.

MAIN RESULTS

```
3.2810640276420684E+00 .....: fmi - Mass flow rate in the entrance (kg/s)
3.2810640276420697E+00 .....: fme - Mass flow rate in the exit (kg/s)
3.3278989266478334E+03 .....: Fd - Dynamic thrust (N)
2.5023386140965442E-16 .....: RESMC - Norm  $L_{inf}$  of the res. of the mass conservation (kg/s)
1.0227000000071712E+01 .....: tcpu - CPU time (s)
```

r189

====

Added subroutine 'save_main_fields' for further comparisons.
Modified 'post_processing_boundaries' subroutine.
Added subroutine 'write_fields_on_boundaries'.
Added subroutine 'plotter07' to plot boundary fields.

MAIN RESULTS

```
3.2810640276420684E+00 .....: fmi - Mass flow rate in the entrance (kg/s)
3.2810640276420697E+00 .....: fme - Mass flow rate in the exit (kg/s)
3.3278989266478334E+03 .....: Fd - Dynamic thrust (N)
2.5023386140965442E-16 .....: RESMC - Norm  $L_{inf}$  of the res. of the mass conservation (kg/s)
9.393999999711290E+00 .....: tcpu - CPU time (s)
```

Test of dt-effect

dt=1e-5

```
3.2810640276420684E+00 .....: fmi - Mass flow rate in the entrance (kg/s)
3.2810640276420697E+00 .....: fme - Mass flow rate in the exit (kg/s)
```

dt=1e-6

```
3.2810640276420346E+00 .....: fmi - Mass flow rate in the entrance (kg/s)
3.2810640276420662E+00 .....: fme - Mass flow rate in the exit (kg/s)
```

dt=1e-7

```
3.2810640276409551E+00 .....: fmi - Mass flow rate in the entrance (kg/s)
3.2810640276421323E+00 .....: fme - Mass flow rate in the exit (kg/s)
```

```

dt=1e-5
 3.3278989266478334E+03 .....:   Fd - Dynamic thrust (N)
dt=1e-6
 3.3279100885934745E+03 .....:   Fd - Dynamic thrust (N)
dt=1e-7
 3.3279100885931780E+03 .....:   Fd - Dynamic thrust (N)

```

The mass flow rate and the dynamic thrust are affected by dt.

```

r190
====

```

The simplified BC for the temperature was implemented.

MAIN RESULTS

```

previous 3.2810640276420684E+00 .....:   fmi - Mass flow rate in the entrance (kg/s)
current  3.2810640276420684E+00 .....:   fmi - Mass flow rate in the entrance (kg/s)

previous 3.2810640276420697E+00 .....:   fme - Mass flow rate in the exit (kg/s)
current  3.2810640276420697E+00 .....:   fme - Mass flow rate in the exit (kg/s)

previous 3.3278989266478334E+03 .....:   Fd - Dynamic thrust (N)
current  3.3278989266478334E+03 .....:   Fd - Dynamic thrust (N)

```

No changes in the mass flow rate and Fd was observed.

The variables u, v, T and p, evaluated at nodes and over the boundaries, were compared with those of r189. The following table shows the maximum relative difference.

Max. relative difference

| Var. | Node | South | North | West | East |
|------|-----------|-----------|-----------|-----------|-----------|
| u | 0.000E+00 | 0.000E+00 | 0.000E+00 | 0.000E+00 | 0.000E+00 |
| v | 0.000E+00 | 0.000E+00 | 0.000E+00 | 0.000E+00 | 0.000E+00 |
| T | 0.000E+00 | 0.000E+00 | 0.000E+00 | 0.000E+00 | 4.094E-03 |
| p | 0.000E+00 | 0.000E+00 | 0.000E+00 | 0.000E+00 | 0.000E+00 |

The only affected variable was the temperature on the east boundary. The relative difference do not exceed 0.5%.

```

r191
====

```

The simplified BC for the pressure deviation was implemented. Pressure extrapolation to fictitious in the 'get_initial_guess' subroutine was changed.

MAIN RESULTS

```

previous 3.2810640276420684E+00 .....:   fmi - Mass flow rate in the entrance (kg/s)
current  3.2810640276420719E+00 .....:   fmi - Mass flow rate in the entrance (kg/s)

previous 3.2810640276420697E+00 .....:   fme - Mass flow rate in the exit (kg/s)
current  3.2810640276420706E+00 .....:   fme - Mass flow rate in the exit (kg/s)

previous 3.3278989266478334E+03 .....:   Fd - Dynamic thrust (N)
current  3.3124021180111745E+03 .....:   Fd - Dynamic thrust (N)

```

No significant change in the mass flow rate occurred, but the dynamic thrust changed by approximately 0.5%.

The results of the current revision (r191) were compared with those of revision r190. The following results were obtained

Max. relative difference

| Var. | Node | South | North | West | East |
|------|-----------|-----------|-----------|-----------|-----------|
| u | 4.181E-03 | 0.000E+00 | 0.000E+00 | 0.000E+00 | 0.000E+00 |
| v | 3.606E-03 | 0.000E+00 | 0.000E+00 | 0.000E+00 | 0.000E+00 |
| T | 1.394E-02 | 8.373E-03 | 1.394E-02 | 5.467E-16 | 1.394E-02 |
| p | 2.094E-02 | 1.152E-02 | 2.094E-02 | 9.518E-16 | 3.611E-02 |

The pressure and the temperature fields were the most affected, with a relative deviation of the order of 3.6%. The velocity fields were changed only on the nodes, with a relative deviation of about 0.4%.

r192
====

The subroutine 'get_p_and_ro_extrapolation_to_fictitious' was implemented. Comparing the results of the current revision (r192) with those of the previous one (r191) it was found the following results

Max. relative difference

| Var. | Node | South | North | West | East |
|------|-----------|-----------|-----------|-----------|-----------|
| u | 1.201E-05 | 0.000E+00 | 0.000E+00 | 0.000E+00 | 0.000E+00 |
| v | 3.988E-05 | 0.000E+00 | 0.000E+00 | 0.000E+00 | 0.000E+00 |
| T | 4.408E-05 | 4.408E-05 | 3.639E-06 | 5.461E-16 | 4.408E-05 |
| p | 5.977E-05 | 5.977E-05 | 6.868E-06 | 4.076E-16 | 1.076E-04 |

The pressure and temperature fields were changed by no more than 0.01%, while the velocities u and v were changed by less than 0.001%.

Test of dt-effect

| dt | | | |
|------|------------------------|-------|---|
| 1E-5 | 3.2810640276420684E+00 | | fmi - Mass flow rate in the entrance (kg/s) |
| 1E-6 | 3.2810640276420662E+00 | | fmi - Mass flow rate in the entrance (kg/s) |
| 1E-7 | 3.2810640276408991E+00 | | fmi - Mass flow rate in the entrance (kg/s) |

| dt | | | |
|------|------------------------|-------|---|
| 1E-5 | 3.2810640276420711E+00 | | fme - Mass flow rate in the exit (kg/s) |
| 1E-6 | 3.2810640276420608E+00 | | fme - Mass flow rate in the exit (kg/s) |
| 1E-7 | 3.2810640276421075E+00 | | fme - Mass flow rate in the exit (kg/s) |

| dt | | | |
|------|------------------------|-------|-------------------------|
| 1E-5 | 3.3124267699298543E+03 | | Fd - Dynamic thrust (N) |
| 1E-6 | 3.3124267699298507E+03 | | Fd - Dynamic thrust (N) |
| 1E-7 | 3.3124267699297829E+03 | | Fd - Dynamic thrust (N) |

The greatest relative difference of the mass flow rate was of the order 1E-13, while the same relative dif. for the dynamic thrust was of the order 1E-14. So, one can say that the dt-effect disappeared.

r193
====

The simplified BC for the velocities u and v were implemented. Comparing the results of r192 with those of r193, it was found the following results

| | | | |
|----------|------------------------|-------|---|
| previous | 3.2810640276420684E+00 | | fmi - Mass flow rate in the entrance (kg/s) |
| current | 3.2812004755405817E+00 | | fmi - Mass flow rate in the entrance (kg/s) |

previous 3.2810640276420711E+00: fme - Mass flow rate in the exit (kg/s)
current 3.2812004755405808E+00: fme - Mass flow rate in the exit (kg/s)

previous 3.3124267699298543E+03: Fd - Dynamic thrust (N)
current 3.3099553704612395E+03: Fd - Dynamic thrust (N)

The mass flow rate had a relative variation of 4E-5 while the the relative deviation of the dynamic thrust was of 8E-4.

Max. relative difference

| Var. | Node | South | North | West | East |
|------|-----------|-----------|-----------|-----------|-----------|
| u | 2.412E-02 | 0.000E+00 | 0.000E+00 | 0.000E+00 | 0.000E+00 |
| v | 5.514E-02 | 0.000E+00 | 0.000E+00 | 0.000E+00 | 0.000E+00 |
| T | 3.407E-04 | 2.122E-04 | 3.407E-04 | 2.658E-05 | 3.407E-04 |
| p | 1.272E-03 | 8.469E-04 | 1.272E-03 | 3.496E-05 | 1.272E-03 |

The u and v fields were the most affected. Their relative deviation do not exceed 6%.

r194
====

The subroutine 'get_Uce_Vcn_at_boundary_faces' was renamed to 'get_velocities_at_boundary_faces'. This subroutine calculates ue, ve, un and vn on the boundaries, besides Uce and Vcn.

Comparing the results of the previous revision (r193) with those of the present one (r194), it was found the following values

previous 3.2812004755405817E+00: fmi - Mass flow rate in the entrance (kg/s)
current 3.2812004755405817E+00: fmi - Mass flow rate in the entrance (kg/s)

previous 3.2812004755405808E+00: fme - Mass flow rate in the exit (kg/s)
current 3.2812004755405808E+00: fme - Mass flow rate in the exit (kg/s)

previous 3.3099553704612395E+03: Fd - Dynamic thrust (N)
current 3.3099553704612395E+03: Fd - Dynamic thrust (N)

There was no difference in the mass flow rate and dynamic thrust.

Max. relative difference

| Var. | Node | South | North | West | East |
|------|-----------|-----------|-----------|-----------|-----------|
| u | 0.000E+00 | Infinity | Infinity | 7.435E-01 | 1.024E-01 |
| v | 0.000E+00 | 0.000E+00 | Infinity | Infinity | Infinity |
| T | 0.000E+00 | 0.000E+00 | 0.000E+00 | 0.000E+00 | 0.000E+00 |
| p | 0.000E+00 | 0.000E+00 | 0.000E+00 | 0.000E+00 | 0.000E+00 |

There were no differences in the pressure and temperature field. The velocities u and v varied only on the boundary faces. This occurred because they were not calculated before.

r195
====

The declaration, allocation and initialization of the variables g was moved to the 'data' module. Removed unnecessary variables pina and plin. Removed unnecessary subroutine 'get_plin_and_p_fictitious' Removed unnecessary variables in the subroutine 'set_bcT'

Comparing the results of the previous revision (r194) with those of the present one (r195), it was found the following values

previous 3.2812004755405817E+00: fmi - Mass flow rate in the entrance (kg/s)
current 3.2812004755405804E+00: fmi - Mass flow rate in the entrance (kg/s)

previous 3.2812004755405808E+00: fme - Mass flow rate in the exit (kg/s)

current 3.2812004755405817E+00: fme - Mass flow rate in the exit (kg/s)

previous 3.3099553704612395E+03: Fd - Dynamic thrust (N)

current 3.3099553704612399E+03: Fd - Dynamic thrust (N)

Max. relative difference

| Var. | Node | South | North | West | East |
|------|-----------|-----------|-----------|-----------|-----------|
| u | 4.173E-14 | 3.720E-15 | 2.603E-14 | 4.023E-14 | 6.626E-16 |
| v | 1.777E-12 | 0.000E+00 | 2.617E-14 | Infinity | 6.414E-14 |
| T | 2.225E-15 | 1.651E-15 | 2.211E-15 | 4.096E-16 | 1.798E-15 |
| p | 9.517E-16 | 9.517E-16 | 6.765E-16 | 4.078E-16 | 6.697E-16 |

The mass flow rate and the dynamic thrust changed by less than 1E-15. The most affected field was the component v of the velocity, that changed by 2E-12, at most. The others fields changed by less than 5E-14.

r196

====

The numerical scheme of the temperature BC on the north boundary was changed in the case of an adiabatic wall. The scheme takes into account the derivatives of T relatively to eta and ksi.

Comparing the results of the previous revision (r195) with those of the present one (r196), it was found the following results

previous 3.2812004755405804E+00: fmi - Mass flow rate in the entrance (kg/s)

current 3.2812004755405804E+00: fmi - Mass flow rate in the entrance (kg/s)

previous 3.2812004755405817E+00: fme - Mass flow rate in the exit (kg/s)

current 3.2812004755405817E+00: fme - Mass flow rate in the exit (kg/s)

previous 3.3099553704612399E+03: Fd - Dynamic thrust (N)

current 3.3099553704612399E+03: Fd - Dynamic thrust (N)

Max. relative difference

| Var. | Node | South | North | West | East |
|------|-----------|-----------|-----------|-----------|-----------|
| u | 0.000E+00 | 0.000E+00 | 0.000E+00 | 0.000E+00 | 0.000E+00 |
| v | 0.000E+00 | 0.000E+00 | 0.000E+00 | 0.000E+00 | 0.000E+00 |
| T | 0.000E+00 | 0.000E+00 | 2.470E-03 | 0.000E+00 | 0.000E+00 |
| p | 0.000E+00 | 0.000E+00 | 0.000E+00 | 0.000E+00 | 0.000E+00 |

The mass flow rate and the dynamic thrust did not change. None of the fields u, v, T and p changed, except T on the north boundary, which changed by less than 0.3%.

r197

====

It was implemented the subroutine 'get_Vce' to calculate the contravariant velocity V on the east boundary. This variable will be used in the calculation of the boundary conditions for u, v, T and p. However, the correct application of this subroutine depends on the calculation of ue and ve on the east boundary. These variables are not updated on the boundaries after the pressure correction. The results of this revision (r197) were compared to those of the previous one (r196) and it was not found any difference.

previous 3.2812004755405804E+00: fmi - Mass flow rate in the entrance (kg/s)

current 3.2812004755405804E+00: fmi - Mass flow rate in the entrance (kg/s)

previous 3.2812004755405817E+00: fme - Mass flow rate in the exit (kg/s)

current 3.2812004755405817E+00: fme - Mass flow rate in the exit (kg/s)

previous 3.3099553704612399E+03: Fd - Dynamic thrust (N)

current 3.3099553704612399E+03: Fd - Dynamic thrust (N)

r198
====

Subroutines 'get_velocities_at_internal_faces_with_pl' and 'get_Uce_Vcn_at_boundary_faces_with_pl' were replaced by 'get_velocities_at_faces_with_pl'. The last subroutine updates the velocities ue, ve, un, vn, Uce and Vcn over interfaces of volumes and over boundary faces.

The subroutine 'get_boundary_simplec_coefficients' was modified so that it gives, due, dve, dun, dvn, besides de and dn.

The calculation of de and dn in the subroutine 'get_initial_guess' was removed, because it was not necessary.

Comparing the results of revision r196 with those of the present revision (r198) it was found the following results

previous 3.2812004755405804E+00: fmi - Mass flow rate in the entrance (kg/s)

current 3.2812004755405830E+00: fmi - Mass flow rate in the entrance (kg/s)

previous 3.2812004755405817E+00: fme - Mass flow rate in the exit (kg/s)

current 3.2812004755405804E+00: fme - Mass flow rate in the exit (kg/s)

previous 3.3099553704612399E+03: Fd - Dynamic thrust (N)

current 3.3099553704612395E+03: Fd - Dynamic thrust (N)

Max. relative difference

| Var. | Node | South | North | West | East |
|------|-----------|-----------|-----------|-----------|-----------|
| u | 3.631E-14 | 5.102E-15 | 3.065E-14 | 2.205E-14 | 8.966E-16 |
| v | 3.061E-12 | 0.000E+00 | 3.074E-14 | Infinity | 1.263E-13 |
| T | 3.142E-15 | 1.379E-15 | 3.278E-15 | 2.734E-16 | 1.402E-15 |
| p | 9.009E-16 | 4.057E-16 | 5.677E-16 | 4.059E-16 | 4.306E-16 |

The relative difference in the mass flow rate and in the dynamic thrust was less than 1E-15.

Among the fields u, v, T and p, the most affected was v, which had a maximum relative deviation of 3E-12. The others variables varied by less than 4E-14.

r199
====

The consistent numerical scheme for the temperature on the east boundary was implemented in the subroutine 'set_bcT'. Comparing the results of the previous revision (r198) with those of the present one (r199), it was found the following results

previous 3.2812004755405830E+00: fmi - Mass flow rate in the entrance (kg/s)

current 3.2812004755405830E+00: fmi - Mass flow rate in the entrance (kg/s)

previous 3.2812004755405804E+00: fme - Mass flow rate in the exit (kg/s)

current 3.2812004755405804E+00: fme - Mass flow rate in the exit (kg/s)

previous 3.3099553704612395E+03: Fd - Dynamic thrust (N)

current 3.3099553704612395E+03: Fd - Dynamic thrust (N)

Max. relative difference

| Var. | Node | South | North | West | East |
|------|-----------|-----------|-----------|-----------|-----------|
| u | 0.000E+00 | 0.000E+00 | 0.000E+00 | 0.000E+00 | 0.000E+00 |
| v | 0.000E+00 | 0.000E+00 | 0.000E+00 | 0.000E+00 | 0.000E+00 |
| T | 0.000E+00 | 0.000E+00 | 0.000E+00 | 0.000E+00 | 2.274E-04 |
| p | 0.000E+00 | 0.000E+00 | 0.000E+00 | 0.000E+00 | 0.000E+00 |

There were not differences in the mass flow rate and dynamic thrust. Among the fields u, v, T and p, T on the east boundary was the only that changed, by an amount of 0.02%.

r200
====

Subroutine 'get_p_and_ro_extrapolation_to_fictitious' was changed in order to implement the consistent numerical scheme for the boundary conditions of p on the north and east boundaries. A subroutine 'get_p_ksi_and_p_eta' was implemented to calculate the derivative of p relatively to ksi on the north boundary and relatively to eta on the east boundary. These derivatives are necessary in the subroutine 'get_p_and_ro_extrapolation_to_fictitious'.

Comparing the results of the previous revision (r199) with those of the current one (r200), it was found the following results

```
previous 3.2812004755405830E+00 .....: fmi - Mass flow rate in the entrance (kg/s)
current  3.2714066384626030E+00 .....: fmi - Mass flow rate in the entrance (kg/s)

previous 3.2812004755405804E+00 .....: fme - Mass flow rate in the exit (kg/s)
current  3.2714066384626066E+00 .....: fme - Mass flow rate in the exit (kg/s)

previous 3.3099553704612395E+03 .....: Fd - Dynamic thrust (N)
current  3.2984290238854687E+03 .....: Fd - Dynamic thrust (N)
```

Max. relative difference

| Var. | Node | South | North | West | East |
|------|-----------|-----------|-----------|-----------|-----------|
| u | 1.007E-01 | 1.907E-03 | 7.051E-02 | 7.705E-03 | 9.532E-03 |
| v | 1.409E+00 | 0.000E+00 | 7.051E-02 | Infinity | 3.041E-02 |
| T | 1.692E-02 | 8.298E-04 | 1.695E-02 | 5.326E-06 | 1.255E-02 |
| p | 1.983E-02 | 3.317E-03 | 1.878E-02 | 1.866E-05 | 7.931E-03 |

The mass flow rate and the dynamic thrust changed by about 0.3%. Among the fields u, v, T and p, v had the greatest relative variation (140%), followed by u (10%), p (2%) and T (1.7%).

r201
====

Subroutines 'set_bcu', 'set_bcv' and 'get_u_v_at_fictitious_nodes_with_pl' were modified in order to apply the consistent numerical scheme on the east boundary for u and v. In the subroutine 'get_initial_guess', the initialization of u and v in the fictitious volumes was done with a extrapolation based on the simplified boundary conditions. A subroutine 'get_phi_eta' was implemented to calculate the derivative of u and v relatively to eta on the east boundary.

Comparing the results of the previous revision (r200) with those of the present one (r201), it was found the following results

```
previous 3.2714066384626030E+00 .....: fmi - Mass flow rate in the entrance (kg/s)
current  3.2714066384626070E+00 .....: fmi - Mass flow rate in the entrance (kg/s)

previous 3.2714066384626066E+00 .....: fme - Mass flow rate in the exit (kg/s)
current  3.2714066384626048E+00 .....: fme - Mass flow rate in the exit (kg/s)

previous 3.3099553704612395E+03 .....: Fd - Dynamic thrust (N)
current  3.2983375254473158E+03 .....: Fd - Dynamic thrust (N)
```

Max. relative difference

| Var. | Node | South | North | West | East |
|------|-----------|-----------|-----------|-----------|-----------|
| u | 6.900E-06 | 1.913E-09 | 9.271E-06 | 2.975E-14 | 1.077E-04 |
| v | 4.699E-05 | 0.000E+00 | 9.271E-06 | Infinity | 1.203E-02 |
| T | 3.092E-05 | 7.010E-09 | 3.153E-05 | 2.734E-16 | 3.166E-05 |
| p | 1.132E-04 | 2.957E-08 | 1.180E-04 | 5.439E-16 | 1.135E-04 |

The the change in the mass flow rate was less than 1E-15, while the dynamic thrust had a

relative variation of 0.35%. Among the fields u , T and p , the greatest relative variation was of 0.01%. The v field varied more. This occur because v is zero or close to zero in some regions, which produces large relative variations.

Referências

- [1] H K Versteeg and W Malalasekera. *An introduction to computational fluid dynamics: the finite volume method*. Longman Scientific & Technical, Harlow, Essex, England, 1995.